Juice-SWI during the Lunar-Earth-Gravity-Assist (LEGA). II. Instrument operations

Thibault Cavalié[1], Raphael Moreno[2], Ladislav Rezac[3], Fabrice Herpin[1], Christopher Jarchow[3], Paul Hartogh[3], Alberto Carrasco Gallardo[3], Samuel Goodyear[3], Pierre Mancini[1], Ali Schulz-Ravanbakhsh[3], Borys Dabrowski[3], Yasuko Kasai[4], Emmanuel Lellouch[2], Axel Murk[5], Donal Murtagh[6], Michael Olberg[6], Miriam Rengel[3], Hideo Sagawa[7], Slawomira Szutowicz[8], and Eva Wirström[6]

[1]Univ. Bordeaux, CNRS, LAB, UMR 5804, F-33600 Pessac, France
[2]LIRA – Laboratoire d'Instrumentation et de Recherche en Astrophysique, Observatoire de Paris, Section de Meudon, 5, place Jules Janssen – 92195 MEUDON Cedex
[3]Max-Planck-Institut für Sonnensystemforschung, Göttingen, Germany
[4]School of Environment and Society, Institute of Science Tokyo, 2-12-1 Ookayama, Meguro-ku, Tokyo 152-8552, Japan
[5]Institute of Applied Physics, University of Bern, Sidlerstrasse 5, Bern, 3012, Bern, Switzerland
[6]Department of Space, Earth, and Environment, Chalmers University of Technology, 412 96 Gothenburg, Sweden
[7]Faculty of Science, Kyoto Sangyo University, Kamigamo-Motoyama, Kita-ku, Kyoto 603-8555, Japan
[8]Centrum Badań Kosmicznych PAN, Bartycka 18A, Warsaw, Poland

Correspondence: Thibault Cavalié (thibault.cavalie@u-bordeaux.fr) and Ladislav Rezac (rezac@mps.mpg.de)

Abstract. The Jupiter Icy Moons Explorer (Juice) embarked in 2023 on a 8-year interplanetary journey to Jupiter and its icy moons. The Submillimetre Wave Instrument (SWI) is one of the ten science instruments aboard the spacecraft. SWI is a sophisticated and first-of-its-kind payload visiting the outer solar system, featuring dual-band tunable receivers, two independent pointing mechanisms, and spectrometers capable of high resolution (up to a resolving power of 10^7). It is designed to support

5 the diverse science objectives of the Juice mission targeting Jupiter's middle atmosphere, icy-moon's exospheres as well as near sub-surface thermophysical properties. For this purpose the Juice mission adopts a complex trajectory tour within the Jovian system, which further necessitates a sophisticated, mission-driven operations concept for SWI. This presents significant planning, operations and commanding challenges which are described in this paper in the context of the Lunar and Earth Gravity Assist (LEGA). After the development and ground calibration of the instrument, the SWI Team has designed a comprehensive

10 calibration strategy applicable during the Cruise Phase of Juice. Among the various opportunities for calibration, including the Near-Earth Commissioning Phase and more than ten Payload Checkout Windows, the LEGA offers the means not only to improve the calibration of the instrument, but also to validate the operational strategy of future icy moon flybys.

1 Introduction

The Jupiter Icy Moons Explorer (Juice, Grasset et al. 2013) is a mission chosen in the framework of the Cosmic Vision 2015-

15 2025 programme of the Science and Robotic Exploration Directorate of the European Space Agency (ESA). Juice was launched on April 14, 2023, from the Kourou space port (French Guiana) and has since embarked on a 8-year interplanetary transfer

to Jupiter, the so-called Cruise Phase. The Cruise Phase is the main mission phase for commissioning, in-flight performance monitoring and calibrating the instruments. Within the three months following launch, the Near-Earth Commissioning Phase (NECP) took place. Payload Checkout Windows (PCWs) are then scheduled on a regular basis and allow instrument teams to

20 check their instrument health for one week every semester on average. The various Earth swingbys do not only offer additional time windows to complement the instrument verification, but they are also unique opportunities to test multi-day planning and observations. The first planetary swingby of the Juice Cruise Phase was the Lunar-Earth Gravity Assist (LEGA), which occurred in August 2024. It will be followed by two other Earth Gravity Assists (EGA) planned in September 2026 and January 2029. In July 2031, Juice will perform its Jupiter Orbit Insertion (JOI) that will start its Jupiter orbital tour. According to the

25 current baseline trajectory (Boutonnet et al., 2024), Juice will then perform a series of Jovian orbits (equatorial and inclined) with 62 perijoves along with 36 moon flybys (2 of Europa, 11 of Ganymede, 23 of Callisto), before performing an orbital insertion around Ganymede (GOI) in December 2034. The final leg of the Juice mission will consist of a suite of elliptical and circular orbits around this icy moon until the end of the nominal mission in late 2035. The Ganymede circular orbits (GCO) will include of high altitude (5000 km), low altitude (500 km), and very low altitude (200 km) orbits.

30 The Submillimetre Wave Instrument (SWI, Hartogh et al. 2026a, b) is one of the ten science instruments aboard Juice. SWI will study the composition, chemistry and dynamics of the atmospheres of the Galilean satellites, as well as their surface properties. It will also investigate the chemistry, dynamics and structure of Jupiter's middle atmosphere and the coupling processes between the planet's atmosphere, its magnetosphere and interplanetary environment. By means of high-resolution (up to $R=10^7$) line spectroscopy and continuum radiometry, it will:

35 - Characterize, in a unique and unprecedented manner, the tenuous atmospheres / exospheres of the Galilean satellites (de Pater et al., 2023; Wirstrom et al., 2020), enabling to determine their sources and sinks (e.g., Marconi 2007), and interactions with the Jovian magnetosphere,

- Measure surface / subsurface properties of icy satellites, constraining thermo-physical properties (e.g., thermal inertia, dielectric constant, porosity) and the surface-bounded atmosphere spatial distribution, composition, and dynam-

40 ics in relation to the exospheres of these bodies (de Kleer et al., 2021),

- Provide a detailed characterization of the thermal field, dynamics, and composition of Jupiter's stratosphere to constrain its general circulation (Cavalié et al., 2021, 2023), and the coupling of the stratosphere with the lower and upper atmosphere (Medvedev et al., 2013; Guerlet et al., 2020; Boissinot et al., 2024),

- Determine key isotopic ratios in Jupiter's and the satellites' atmospheres, constraining the origin and evolution of

45 the jovian system (Mousis et al., 2014; Gapp et al., 2024; Lefour et al., 2026).

SWI is a heterodyne radiometer/spectrometer operating in two different submillimetre channels using two independent local oscillators (LO) to observe the sky simultaneously at two wavelengths, 233-281 μm (1066-1286 GHz) and 470-565 μm (530-638 GHz), with selected spectrometers. It can record the sky emission over two spectral windows, either with very high spectral resolution Chirp Transform Spectrometers (CTS, 1 GHz bandwidth, 10000 channels, 100 kHz resolution), the high resolution

50 Auto-Correlation Spectrometers (ACS, 4.4 GHz bandwidth, 1024 channels, 4.3 MHz resolution), or with the Continuum Chan-

nels (CCH, 4 GHz bandwidth). The CCH can be used as stand-alone or in combination with either the ACS or the CTS. SWI is a miniaturized observatory aboard Juice, comprising a Telescope and Receiver Unit (TRU), an Electronic Unit (EU), and a radiator. The TRU has a main antenna with a diameter of 29 cm. The instrument TRU is equipped with two orthogonal pointing mechanisms that allow to point to any position in the sky from the nadir direction of the Juice platform with a freedom of $\pm72°$

55 along track (AT) and $\pm4.3°$ cross track (CT) during the Jupiter orbital phase of the Juice mission. It also bears a flip mirror (FLM) that enables switching from an optical path pointing to the sky to another path pointing to an internal calibration hot load.

SWI is thus a complex instrument that requires a comprehensive calibration plan, similarly to other heterodyne instruments flown on submillimetre observatories, like the Heterodyne Instrument for the Far-Infrared of Herschel (Roelfsema et al., 2012)

60 or the receivers of Odin (Olberg et al., 2003). This plan aims to understand the instrument's stability, spectral and spatial responses, enable proper radiometric calibration of the data, etc., and to track the temporal evolution of all these parameters. It is described in Hartogh et al. (2026a). SWI stands out uniquely in its complexity from the science plan perspective. Unlike missions/instruments such as Odin, Herschel, or Rosetta/MIRO (Microwave Instrument for the Rosetta Orbiter), where target and orbital scenarios remained relatively stable, the science phase of SWI involves dynamically changing targets and orbits,

65 thereby science goals. This evolving operational context introduces a level of challenge and adaptability that was not present in previous missions, making the SWI planning and execution significantly more intricate. To execute the calibration and science plan, the sub-units of the instrument need to be commanded by its Digital Processing Unit (DPU) in order to build calibration observations and observations of science targets. Section 2 presents the concept and description of the observation modes which are used to operate the instrument. Section 3 details the concept of SWI operations planning. Finally, section 4 exposes

70 the overall observation strategy of SWI for the Cruise Phase.

2 Observation modes

SWI operates with two hierarchical levels of modes. First, there are the instrument modes, a term which is used to communicate the highest level of controlling of the instrument with the onboard application software. Second, there are the observation modes. The observation modes, as will be discussed, are encapsulated and can be also referred to as "scripts"/"science scripts".

75 They can be invoked with parameters when the instrument is running in its "science" instrument mode. These two types of modes are described in this section.

2.1 Instrument modes

There are 6 basic instrument operational modes that can be commanded with the SWI application software:

- OFF: All instrument subsystems including the DPU are switched off. Consequently, there is no housekeeping data

80 and no telemetry generated by the instrument itself. The instrument is in this mode during launch and Cruise Phase, except during calibration campaigns (e.g., NECP, PCWs, Earth and Moon flybys).

- STANDBY: Only the instrument DPU is switched on and is able to receive instrument commands. Only housekeeping telemetry is generated in this mode.

- SAFE: The DPU and ultra-stable oscillator (USO) are switched on. This mode is used in different cases. It serves for the USO stabilization prior to warm-up. It is also the mode into which the instrument switches automatically in case an instrument anomaly is detected. SWI is also switched to this mode at the end of science operations and is meant to be used during downlink. Only housekeeping telemetry is generated in this mode.

- DIAGNOSTIC: The DPU, USO, and selected spectrometers (CTS or CTS/CCH or ACS or ACS/CCH) are switched on. Diagnostic activity is allowed in this mode, including activation and control of sub-units.

- UNLOCK: Only the DPU is switched on. This mode was only used once post-launch to release the launch locks of the instrument mechanisms that kept the TRU in its launch position.

- WARMUP: The DPU, USO, and selected spectrometers (CTS or CTS/CCH or ACS or ACS/CCH) are switched on. This mode is a transition mode to enter the SCIENCE mode.

- SCIENCE: The DPU, USO, and selected spectrometers (CTS or CTS/CCH or ACS or ACS/CCH) are switched on. This mode serves to invoke calibration and science observations with the appropriate list of mode parameters (see next Section).

The allowed transitions between these instrument modes are illustrated Fig. 1.

2.2 Concept of observation modes

During the Science Phase (Jupiter tour and Ganymede orbits), Juice will operate on the basis of 16 hrs of science operations per day, followed by 8 hrs for communications with the Earth ground stations (downlink and uplink activities). Because of telemetry budget limitations, ESA has defined the number of 100 telecommands (TC) as the limit for uplink per science day per instrument. This limit makes it impossible to operate SWI with individual sub-unit commands, because a single science observation lasting just a few minutes would already require tens to hundreds of those commands. An observation indeed requires several steps to be taken, like the tuning of the receivers, setting the pointing mechanism, pointing to the science target, performing the required ON-OFF integrations (including pointing to the cold sky for OFF integrations), and making the relevant hot-cold calibration integrations (including the relevant FLM movements). Even the simplest observation, i.e., a nadir stare without any repetition of the integration loop, requires a minimum of 16 commands. Early in the development phase of the instrument, it was therefore decided by the instrument team to adopt the concept of observation modes, similarly to Herschel-HIFI (Roelfsema et al., 2012). These are a set of scripts, pre-loaded in the DPU memory, that can be invoked by single TC, once the instrument is set in the SCIENCE Mode. Each script is a suite of sub-unit commands, which can be grouped in repetition loops, in order to produce a complete observation (e.g., 2D map). The details of the operation of each single script execution are then uniquely governed by the list of parameters supplied by the TC.
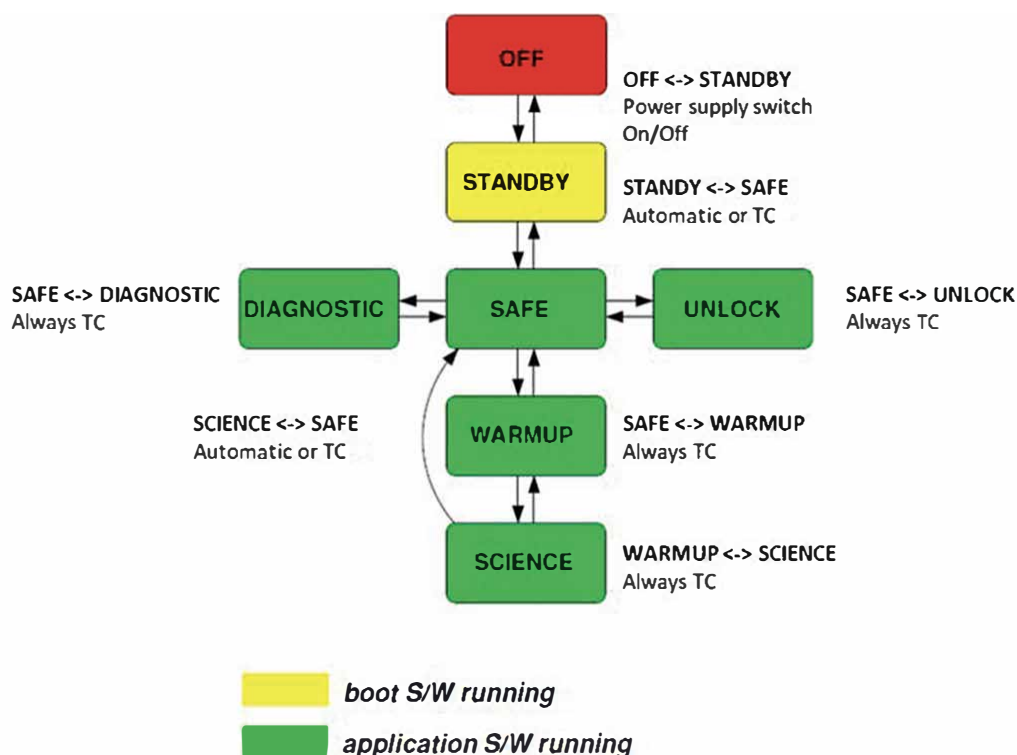
Figure 1. Transitions between instrument modes in the SWI DPU. Science observations are performed when the instrument is set to its SCIENCE mode. Credit/property of MPS.

2.3 General description

SWI currently has a total of 34 observation modes implemented in its DPU. Observation modes can be grouped in two cate-
115 gories: calibration modes meant for characterization and monitoring of the instrument and its behavior, and science observation modes meant for science measurements. A mode/script is fully defined by a set of parameters which concerns, for example, tuning, receiver and spectrometer setup, mechanism movements for pointing. All modes are provided with details in the Appendices A and B.

2.3.1 Calibration modes

120 There are 9 calibration modes for SWI. They have been designed to characterize the Allan variance and to measure the system temperature with all backends (CTS, ACS, CCH). The Allan variance modes (all modes with names starting with "SWI_-ALLAN", see Appendix A) use the shortest integration time possible and accumulate integration time in order to characterize up to which integration time the spectral noise decreases according to the radiometric formula (Schieder and Kramer, 2001). It can be applied to any of the possible tunings of the instrument. The radiometric formula links the spectral noise with the

125 integration time of an observation and requires the knowledge of the system temperature (Tolls et al., 2004; Gulkis et al., 2007). The system temperature modes (all modes with names starting with "SWI_TSYS", see Appendix A) consist of a spectral scan across several tunings that can be supplied via the TC. For instance, the system temperature mode using the CTS can cover up to 15 tunings in each band. The SWI mechanisms may be used to point SWI beam to the cold sky at the start of all these calibration modes. However, the mechanisms are not used during the actual measurements.

2.3.2   Science observation modes

To cover all the science objectives of the instrument, the SWI Team has defined a total of 22 science observation modes. The science observation modes are distinct by their pointing pattern, which have been carefully designed to match all the observation requirements derived from the instrument science goals (Hartogh et al., 2026a). All modes contain repetition loops, i.e., sequences that enable the accumulation of integration time on the selected target (single point or maps).

135 The generic science modes enable the observation of a target either with: (i) a nadir stare (all modes with names starting with "SWI_NADIR_STARE", see Appendix B), with the possibility to define an offset to the nadir position to aim for a particular latitude/longitude/region-of-interest of the target (e.g., Stephan et al. 2021 for Ganymede), (ii) a 5-point cross for low spatial resolution mapping (all modes with names starting with "SWI_5POINT_CROSS", see Appendix B), (iii) a 2D map consisting of evenly separated rows and columns (all modes with names starting with "SWI_2D_MAP", see Appendix B). The 2D maps

140 are very versatile and can be customized to many different purposes by setting the proper parameter values. For instance, the 2D map mode can serve to perform a zonal (resp. meridional) scan by setting the number of rows (resp. columns) to one. Also, the separation between two consecutive rows can differ from the separation between two consecutive columns in a 2D map. The observation principle of these modes is shown in Figs. B1 and B2.

Most of the science observation modes are defined for use with the CTS simultaneously with the CCH. All these modes

145 enable single or (preferentially) dual band observations of a target, by defining one or two tunings. They can also be used either based on the position-switching calibration technique, where the instrument alternates between the science target and the cold sky to achieve radiometric calibration of the measurements, or based on the frequency-switching technique, where the LO is tuned to a nearby frequency to perform the radiometric calibration. The latter is generally used for the observation of narrow lines (Hartogh et al., 2010a; Biver et al., 2015) and enables spending nearly 100% of the integration time on the target, provided

150 that the spectral lines are significantly narrower than the LO frequency throw applied in the scheme. The 2D map mode also comes in an on-the-fly version (all modes with names starting with "SWI_2D_MAP_OTF"), in which a cold sky measurement is taken only once at the end of each row of the map (Ossenkopf 2009, and see examples of applications in Gallardo Cava et al. 2023 and Szabó et al. 2025). The cold sky measurement ending a row is then applied to all the on-source points of that same row, instead of being recorded after each on-source point of the row when using the position-switching version of the

155 mode. The duty cycle is then largely improved, provided that the instrument is stable enough (i.e., the instrument gain drifts are negligible) over the duration of a row.

In addition, spectral scan modes (all modes with names starting with "SWI_SPECTRAL_SCAN", see Appendix B) have been defined for use either with the CTS or with the ACS, either with the position-switching calibration scheme or with the

frequency-switching scheme. These spectral scans enable to observe many tunings in one execution (see example in Costagliola

160   et al. 2015; De Beck and Olofsson 2018), for instance, 15 tunings for the spectral scan with the CTS and position-switching. Similarly to the nadir stare modes, the spectral scans are nominally nadir, but can be offset to any region of interest of a target (e.g., limb direction).

Using the capabilities of SWI, target-specific science observation modes have also been designed to maximize the science return of the Jupiter and moon observations. One of the main science goals of the instrument is to constrain the general

165   circulation in the stratosphere of Jupiter. It is thus crucial to measure temperature and winds preferably simultaneously with the required accuracy to constrain the mechanical forcings at play in the atmosphere (Hartogh et al., 2026a). This is best achieved with limb observations of the CH_4 lines at 1256 GHz and a strong line in the 600 GHz band, like the H_2O line at 557 GHz. Alternately, a strong H_2O line can be used in the 1200 GHz band. However, the vertical range over which the temperature can be retrieved is then more limited, because H_2O is restricted to the upper and middle stratosphere by condensation (Moses et al.,

170   2005; Cavalié et al., 2008). In all cases, the retrieval of the winds necessitates to know where the instrument pointed to enable the subtraction of the beam-convolved planet rotation with an accuracy better than the wind accuracy required to constrain the models(Cavalié et al., 2021; Benmahi et al., 2022, 2025; Carrión-González et al., 2023), because the Doppler shift induced by typical stratospheric winds of 100 m.s^{-1} is superimposed on a much larger Doppler shift induced by the 12.5 km s^{-1} planet rotation. To achieve such accuracy in the limb pointing determination, each limb integration with the CTS is preceded by a rapid

175   scan across the limb with the CCH. When the recorded signal reaches 50% of the nadir signal, the instrument boresight is at the limb. The scan is thus stopped and the integration with the CTS starts. This can be programmed either for a single latitude (all modes with names starting with "SWI_JUP_LIMB_STARE", see Appendix B) or for a series of latitudes (all modes with names starting with "SWI_JUP_LIMB_RASTER", see Appendix B). The observation principle of these modes is shown in Fig. B3. These modes are also to be used for deep integrations that aim at detecting isotopes and trace species, because an accurate

180   pointing at the limb maximizes line contrast, which is especially crucial for faint lines. For temperature/wind measurements, the position-switching version of the mode will be used, because the targeted lines are broader than the frequency throw enabled in the frequency-switching modes. For isotopic lines and the search for new species, the frequency-switching version may be used, provided that the temperature information is not needed (because already obtained for the pointed latitude/longitude).

For the investigation of Galilean moons subsurface, atmospheric abundance, composition and temperature, there are spe-

185   cific nadir stare modes (all modes with names starting with "SWI_MOON_NADIR_STARE", see Appendix B). The only difference with the generic nadir stare mode described above is the addition of CCH measurements recorded in parallel of the CTS ones. During a given CTS integration (generally 10-60 s), CCH measurements are taken in parallel, with a much shorter integration time (generally 0.4 s), and thus with at a higher cadence. This significantly improves the spatial sampling of the surface/sub-surface temperature, and thus facilitates moon surface science from those continuum measurements, without

190   impacting significantly the total data volume. For winds, temperature, isotopes and trace species, there are two types of limb modes. For deep integrations, one can use the limb stare mode (all modes with names starting with "SWI_MOON_LIMB_-STARE", see Appendix B), that enables to point at a given latitude and altitude. For temperature, composition and wind vertical profile sampling when the beam is smaller than the apparent width of the atmospheric limb, limb scanning will be preferred

(all modes with names starting with "SWI_MOON_LIMB_SCAN", see Appendix B), similarly to how Guerlet et al. (2018)
195 operated Cassini/CIRS (Composite Infrared Spectrometer) on Saturn. This mode enables to target a latitude and to scan up and
down from the surface to the top of the atmosphere, with an altitude step that is adaptable to the science goal. The observation
principle of both limb modes is shown in Fig. B4.

2.4 Validation of the observation modes

The details on how to execute a given science observation have been defined partly based on theory and partly on experience
200 from other microwave or infrared instruments in space (e.g., Roelfsema et al. 2012). It is necessary first to verify if the scripts
are functional on the ground and then to test inflight if these observation modes provide science data with the expected quality.
This mode validation thus constitutes part of the Cruise Phase operations of SWI.

2.5 Summary on observation modes

SWI is an instrument aiming to observe surfaces and atmospheres in the Jovian system to measure composition, temperature
205 and wind speeds. To achieve all these goals, the instrument was designed with all the flexibility (and complexity) as that
found in ground-based sub-mm observatories, including, for instance, pointing pattern, spectral tuning, coverage and sampling,
integration times, integration repetition factors, etc. All the calibration and science observation modes described in Section 2.3
can be fed with the appropriate parameters to match a given measurement goal. Each observation is thus unique and must not
only use one of the modes with the appropriate list of parameters, but it must also carry a series of metadata that provide the
210 necessary information to enable meaningful data reduction and analysis. The description of the concept of operations of SWI
is given in the next section.

3 Observation planning during the LEGA

3.1 Generalities on observation planning

The planning of operations during any of the Cruise Phase opportunities, including the LEGA, follows several steps. In a first
215 step, the Mission Operation Center (MOC) defines the boundary conditions of the operations: date/time, duration, allowable
data volume, etc. Instrument teams are then asked for a preliminary Activity Plan (APL) with operation names and descrip-
tions, estimates of number of TC, duration and data volume, and applicable constraints. MOC usually proposes a preliminary
breakdown of the data volume envelopes per instrument. In a second step, instrument teams submit an initial sequence of op-
erations, in the form of a preliminary list of Payload Operation Requests (POR). At this stage, there can be trade-offs between
220 instruments, managed by MOC. Once the final envelopes are agreed upon, the teams are requested to submit their final PORs
several weeks before execution of the operations.

During the Science Phase, iterations with instrument teams are managed by Science Operation Center (SOC, Altobelli et al.
2026). SOC initially provides a segmentation of the trajectory, which prioritizes operations on a science-driven basis. SOC

then handles the various instrument team deliveries, starting with the Observation Plan (OPL). The OPL is a list of instrument observation requests, which are backed up by a science plan. Instrument teams can request observations under two statuses: prime or rider. The prime status implies the instrument has constraints on the spacecraft pointing, while the rider status bears no such implication. After harmonization of the OPLs from all the instrument teams, a skeleton spacecraft Pointing Timeline Request (PTR) is generated and SOC designates which instrument team has to design the spacecraft pointing for each time block of the timeline. Once the final PTR is produced, SOC provides a skeleton Instrument Timeline (ITL), which provides the information on spacecraft resources (power, data rate and data volume). Some operations can then still be removed to comply with, for example, the total power available to instruments at a given point on the timeline.

Because the LEGA operations were managed by MOC, and because there was no spacecraft pointing allowed during the whole LEGA timeline, the setting of the whole timeline of operations did not necessitate to go through the various steps that will be required in the Science Phase. Some trade-offs had to be found for the closest approaches to the Moon and the Earth, but, as will be discussed in the next sections, almost only SWI operations occurred in the days following the closest approach to the Earth, because it was the only instrument that could point to the Earth and Moon with its mechanisms.

3.2 Specificity of SWI observation planning

The planning of SWI observations requires accurate pointing information that relies on the interpretation of the mission SPICE (Spacecraft, Planet, Instrument, C-matrix, Events) kernels[1], which are regularly updated and delivered by ESA. This is true for all modes except the calibration modes.

Geometrical calculations derived from the SPICE kernels must be performed individually for each script in order to obtain accurate pointing information for the observations to be scheduled. Other target-specific geometric information that cannot be derived a posteriori from the commanding parameters such as, for instance, target name, target size, sub-spacecraft latitude and longitude, and local time, must also be included in the metadata of an observation.

In practice, the metadata of an observation are not uplinked to the spacecraft. Only the list of TCs containing the sequence of observation modes with their relevant list of parameters is sent for operation execution. For a given observation, those metadata, the selected observation mode and the parameter list are kept in a database of planned observations. They are used upon the downlink of the telemetry binary files (both housekeeping and science data) by the SWI telemetry-to-raw (TM2RAW) pipeline to automatically create the proper file structure and to populate it with the raw data. A high-level description of the SWI TM2RAW pipeline is shown in Fig. 2. This is absolutely necessary, because, for example, the binary data file from a 60-minute 2D map with 10×5 on-source points with 5 s integration time per point will have a different structure and contain a different amount of data (e.g., number of spectra) compared to a 10-minute nadir stare. A second implication is that each calibration and science observation mode must have its dedicated data reduction pipeline.

Consequently, the SWI Science Team has opted for a unique observation identification number for each planned observation, similarly to what was made for Herschel observations (e.g., Hartogh et al. 2010b, Cavalié et al. 2013, 2014). These so-called ObsIDs (observation identification numbers) serve this purpose of tailoring an observation, defined by its observation mode

---

[1]https://www.cosmos.esa.int/web/spice/spice-for-Juice
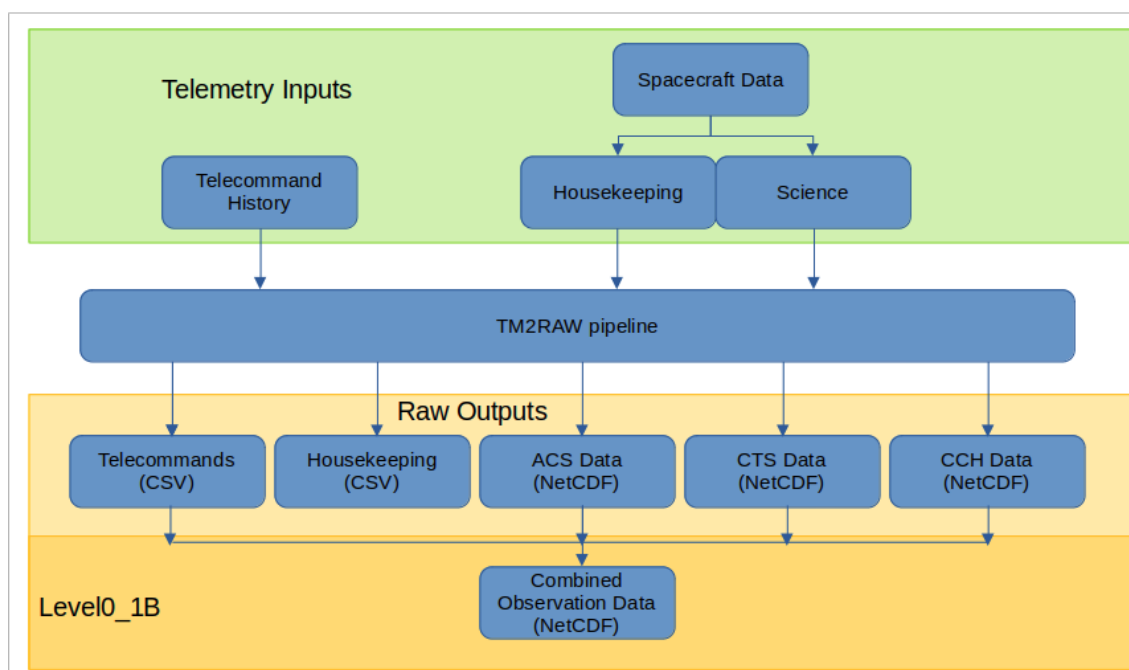
Figure 2. Flowchart representing the SWI processing of spacecraft telemetry packets into raw data files, and subsequently into Level0_1B which additionally include the necessary telecommanding metadata. This is a high-level outline of the SWI telemetry-to-raw (TM2RAW) pipeline. The formats of the various output data produced by the TM2RAW pipeline are specified within parentheses. The Level0_1B files are then inputs into the SWI calibration pipeline.

and list of parameters, with its mandatory metadata from the planning stage down to the data reduction stage. They uniquely identify, characterize and naturally encapsulate the SWI data/observations. We should also highlight here that SWI data will be calibrated and archived in chunks identified by the ObsIDs.

3.3 The SWI Observation Planning Tools

The preparation of the planning and uplink file deliveries by the SWI Team follow slightly different process for ongoing Cruise Phase operations and the future Science Phase after the JOI. This distinction is driven by external procedural approaches of MOC and SOC that are required during the different phases. Nevertheless, for SWI there is a strong overlap, also in the software used to produce the necessary commanding files and meta-data. In general, SWI planning relies on the selection of observations based on science priorities, and on the subsequent computation of the instrument parameters for each of the selected observation and corresponding observation mode. This is achieved with a suite of observation planning tools, which are described in the following sections. They constitute the SWI Commanding pipeline. The full flowchart summarizing the various steps from the initial inputs to the submission of PORs is shown in Fig. 3.
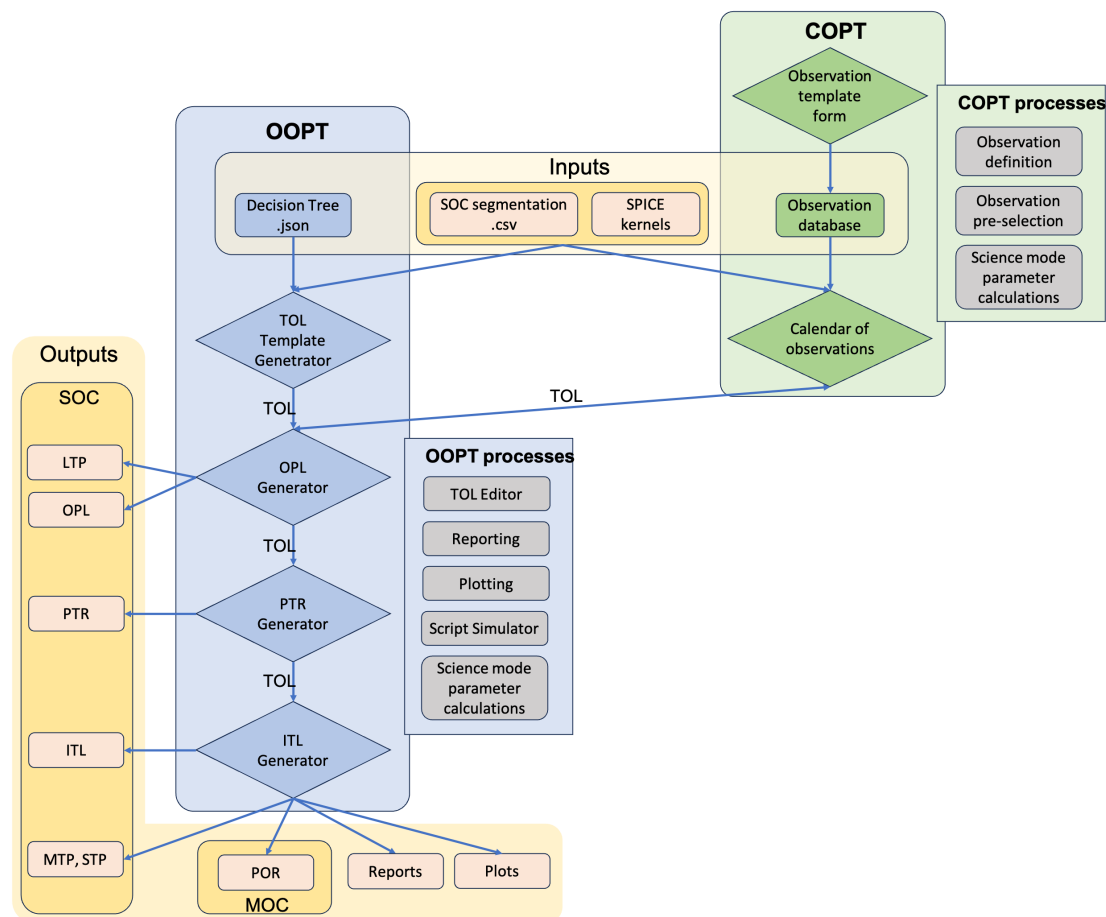
Figure 3. Flowchart representing the various steps required from initial inputs (e.g., SOC segmentation, SPICE kernels) to the various deliveries (e.g., MTP, LTP, PORs) in the Science Phase. The Science Co-Is start with the preparation of a calendar of science observations using the COPT to produce an initial TOL for the OOPT. The Operator then produces the initial OPL, and verifies the possibility to execute the Plan with the Script Simulator. After harmonization with SOC, the PTR is produced and harmonized. Finally, the ITL is produced and harmonized. This concludes with the production of the PORs with the computation of the script parameters for each observation. At every intermediate step, the OOPT can produce reports, plots, etc.

3.3.1 The Co-I Observation Planning Tool (COPT)

270 The main goal of the COPT is to provide the Science Team with the means to produce a high level schedule of the SWI observations (inflight calibration and science observations). This primarily concerns the mid-term plan (MTP). As such, the LEGA can be considered as the first inflight MTP with the whole Juice payload. The COPT is a web-based tool accessible

to the instrument co-investigators (Co-Is), to allow them to prepare and propose observation schedules relevant for the MTP stage. The COPT consists of:

275
- a database of observations with all the properties that define them: target, expected duration, observation mode, pointing properties, selected spectral lines, spectrometer parameters, etc. This database shall contain several hundreds to thousands observations for the complete Science Phase of the mission.

- a database of geometrical data computed from the mission SPICE kernels: target sizes, position and orientation with respect to the Juice and SWI reference frames, radial and tangential velocities relative to Juice and to the SWI 280 boresight, etc.

- a calendar in which the observations are scheduled.

- a set of scheduling rules to preselect the observations that are feasible at any given point in time of the mission.

- algorithms to compute the relevant instrument parameters and resources (execution time, power, data rate, and data volume) for each scheduled observation. A non-exhaustive list of parameters that are calculated, and subsequently 285 appended to the invocation of an observation mode in a TC, comprises: the tuning indexes for one, the other or both bands; the number of spectral channels (for the ACS) or the start and end channels (for the CTS); a spectral binning factor (for the CTS); activation switch of the CTS comb (for the calibration of the frequency scale); choice of mechanism end-switches for pointing initiation; number of AT and CT steps to the sky position, to the target and to the external hot load (when applicable); mapping or scanning AT and CT steps; frequency throw (for frequency- 290 switching modes); ON and OFF integration times for the CTS or the ACS and/or the CCH. Finally, loop counters and timing delays between subsequent commands are computed to match at best the expected observation duration, which is derived from observation simulations (so as to reach a given signal-to-noise ratio). It also produces the list of required metadata, that includes: version of SPICE kernels, observation start time stamp, total execution time, total power, total energy, number of measurements (CTS, ACS and CCH), data volume, data rate, distance to the 295 Sun, target identifier, target geometrical properties, etc.

The output produced by the COPT is list of time stamps, observation mode invocations with appropriate list of parameters and corresponding metadata. Essentially, it is a draft of what we termed a time-ordered-list (TOL) of SWI operations. With this information the SWI operators enter into the "harmonization" process which iterates with MOC (during the Cruise Phase) or SOC (during the Science Phase) to account for external spacecraft or other instrument constraints on, for example, power, 300 pointing, data volume and etc. to achieve the final scheduling of SWI observations. Because the number of scheduled SWI observations, each of which being unique due to the input parameters, can reach up to several hundreds, the final harmonization is achieved with another software, the Operators Observation Planning Tool (OOPT).

3.3.2 The Operator Observation Planning Tool (OOPT)

The OOPT is a software designed to assist with the MOC/SOC harmonization process and ultimately produce the various files
305 necessary for the preparation of the delivery of the planning files to ESA (MOC or SOC). This tool comprises the following
features:

- A helper procedure to fully populate the TOL that uses a set of predefined scheduling rules ("Decision Tree" in
  Fig. 3), the segmentation proposed by SOC, and the SPICE kernels. It produces a generic TOL for the purpose of
  preparing the Long-Term Plan (LTP). This TOL can be imported into the COPT to provide scheduling guidelines to
310   the Science Co-Is for further refinement.
- A TOL editor that the operator can use during the various harmonization stages to adapt the timeline of operations.
- A series of functionalities that enable plotting and reporting on the various operations of the TOL.
- A script simulator, which purpose is to provide the following information on what a given observation mode/script
  will do with the provided parameters:

315   - check the entire execution with timings and check that the script will execute properly
- accumulate AT, CT and FLM motor movements, information that is also stored for lifetime monitoring
- provide instantaneous AT and CT motor steps, which are converted to angular offsets and define the
  planned SWI pointing.
- provide instantaneous as well as accumulated execution time of a script for double checking against
320   COPT results
- estimate average data rate (DR) and the total expected data volume (DV).

Furthermore, it is during the OOPT process that a unique ObsID is assigned to each of the scheduled observations.

3.3.3 Conclusion on the SWI OPTs

Both the OOPT and COPT, along with their generated products, are continuously being validated with the ongoing Cruise Phase
325 operations. This is particularly true in dedicated SWI pointing observations conducted during the Near-Earth Commissioning
Phase, the initial Payload Checkout Windows, and the LEGA campaigns. These activities have been instrumental in refining
and achieving fully functional, integrated OPTs across all observation modes.

4 Observation strategy for the LEGA

4.1 Context

330 The Cruise Phase of Juice began right after its successful launch on April 14, 2023. It will last for about 8 years, until its arrival
at Jupiter in July 2031. The evolution of angular sizes of the Sun, Venus, the Earth, Mars, and Jupiter, as seen from Juice during
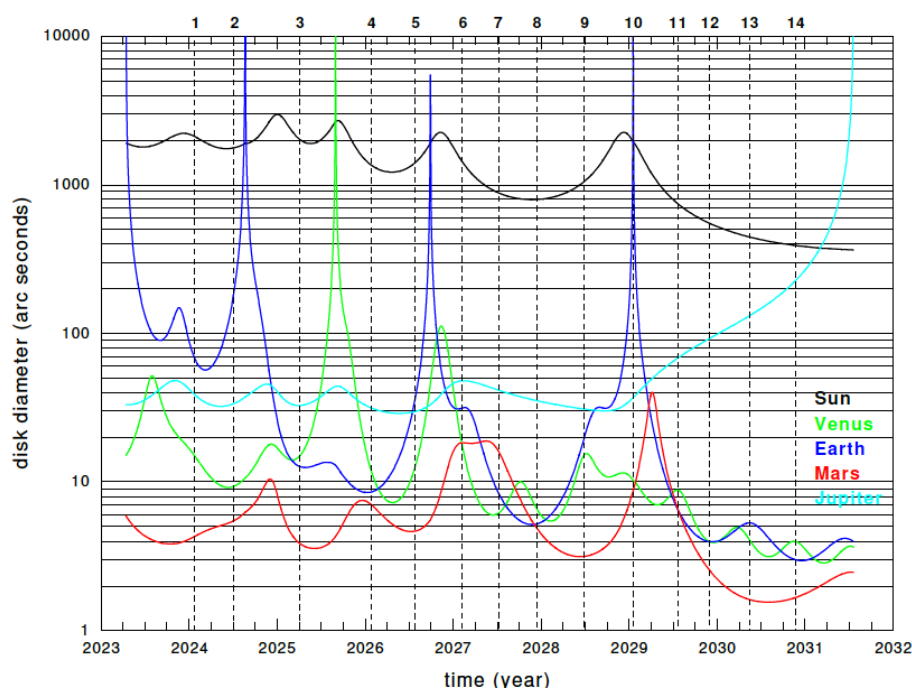
Figure 4. Angular sizes of the Sun (black line), Venus (green line), the Earth (blue line), Mars (red line), and Jupiter (cyan line), as seen from Juice during the Cruise Phase. The different PCWs are labeled on the upper x-axis at their corresponding epoch.

the Cruise Phase, are shown in Fig. 4. The first three months were used to commission the spacecraft and its instruments, during the NECP. The subsequent long interplanetary phase leading to Jupiter Orbital Insertion (JOI) comprises several regular Payload Checkout Windows, meant for periodic functional checks of instruments, performance verification and calibration. It

335 also involves four planetary flybys to send Juice to Jupiter (Boutonnet et al., 2024). These gravity assists enable controlled deviations in the spacecraft's trajectory, ultimately placing it into a heliocentric orbit tangential to Jupiter's orbit by July 2031, ensuring a successful JOI.

From the planning and operational point of view the Earth gravity assists manoeuvres provide great analogues for future Galilean moon flybys, testing SWI's relevant operational timelines. The first of these encounters, the LEGA, occurred in

340 August 2024 and was actually a double gravity assist, with a flyby of the Moon on August 19, 2024, with a closest approach altitude of about 700 km, followed 24 hours later by a flyby of the Earth, with a closest approach altitude of about 6800 km. Further payload operations were possible in the three days that followed the closes approach to the Earth. In total, the LEGA segment resulted in the execution of a total of 166 observations by SWI (for 225 observations planned).

The general strategy for the combined flybys was three-fold: (i) to validate in representative close flyby operating conditions

345 the use of several key observation modes, (ii) to perform spectral, and spatial calibration observations using SWI's own pointing utilizing known strong lines and/or continuum, and (iii) search for new lines in the Moon exosphere and in the Earth atmo-

sphere. It should be noted that it was the first time the atmosphere of the Earth was observed at frequencies around 1200 GHz. A general overview of the Moon and Earth observations is provided in the next sections.

4.2 Moon flyby

350 The key characteristics of the Moon flyby in the context of SWI pointing are shown in Figs. 5 and 6. The spacecraft attitude commanding around ±50 min the closest approach were restricted to keep optimal conditions for the geophysics (in-situ) instruments. The +Z axis of Juice was fixed essentially in a nadir view during this period. Because the lunar distance changed very rapidly near closest approach, it was not feasible to perform extensive mapping of the Moon's emission across different latitudes and longitudes or to evaluate the SWI limb-staring, scanning, or mapping modes. Therefore, we opted for an

355 unconventional use of the SWI_2D_MAP_OTF_V1 around closest approach, by manually setting the instrument antenna in its nadir direction (aligned with spacecraft +Z axis), commanding only a single map row, and setting mechanism offsets to zero in-between subsequent raw points so as to keep the antenna pointing unchanged. Furthermore, implementing the shortest possible integration time for the CTS, i.e., 1.5 s, and defining a large "map" size has effectively enabled us to record a full track of measurements while the Moon drifted below SWI and the spacecraft during the flyby. The use of the OTF mapping mode

360 for this observation (ObsID 227) also bore the advantage of avoiding antenna movements for the cold sky position in-between two subsequent integrations.

Once the Moon eventually moved out of the field-of-view (FOV) of the instrument, a second execution of this observation was scheduled. ObsID 228 required repointing the SWI antenna by 54° back (against the direction of the spacecraft velocity vector) using the AT mechanism. By doing so, SWI kept recording Moon spectra for approximately 45 additional minutes. For

365 both ObsIDs (227 and 228), we tuned the receivers to the frequencies of the H_2O lines at 557 GHz and 1113 GHz to test those tunings, because they are crucial for the Jupiter and Galilean moon observations during the Science Phase.

The Moon flyby observations are summarized in Table C1 of Appendix C. The science goals and results are presented in Rezac and et al. (2026).

4.3 Earth flyby

370 Similarly to the Moon flyby, the Juice remote sensing instrument platform (the +Z platform) maintained a near-nadir pointing orientation for several minutes around its closest approach to Earth. During this time SWI performed four observations (ObsIDs 229-232, see Table D1 in Appendix D), two on either side of the closest approach. The first and fourth were similar to those executed during the Moon flyby, i.e., two strips of SWI_2D_MAP_OTF_V1 mode manual setup. Key characteristics and the timing of the four SWI observations are shown in Fig. 7.

375 The first observation used nadir pointing of the antenna, while the fourth observation (post-closest approach) required to repoint the antenna towards the Earth. In both cases, the receivers were tuned to the frequencies of the H_2O lines at 557 GHz and 1113 GHz to further test those tunings with a target atmosphere that contains H_2O. It should be noted that many other lines were also potentially detectable in the spectral windows covered by those two tunings.
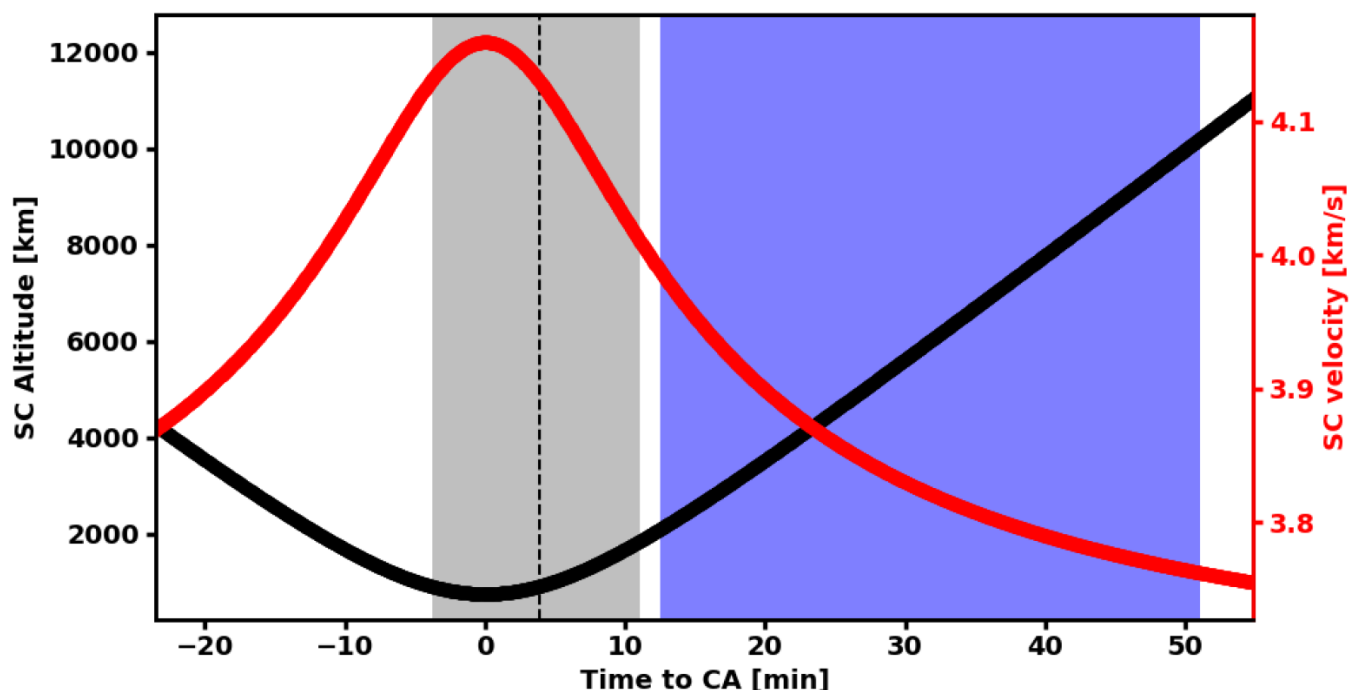
Figure 5. Juice altitude in km (black line) and relative velocity in km s^{-1} (red line) around the closest approach during the Moon flyby, on August 19, 2024. The gray and blue (respectively) areas represent the time windows during which the ObsIDs 227 and 228 (respectively) were recorded, i.e., when SWI had the Moon in its FOV. The black dashed line indicates the terminator crossing, and the gap between the two filled areas shows the time required to switch from the first to the second observation and move the SWI antenna back to the Moon with the AT.

The second observation, just before the closest approach, benefited from the largest relative size of the Earth atmospheric limb. Because this maximized the potential for detection of weak lines, the SWI team designed a limb scan using SWI_-MOON_LIMB_SCAN_PS_V1, with the receivers tuned to an HDO line. This observation also enabled the validation of the use of this mode in a close flyby situation. The third observation, just after the closest approach, was designed with the SWI_MOON_LIMB_STARE_PS_V1 to observe another couple of weak lines from $H_2^{17}O$ and $H_2^{18}O$, and also enabled the validation of using this mode in close flyby operating conditions. For both observations, we chose to compute the relevant pointing parameters (tangent altitude for the limb stare, altitude range and steps for the limb scan) for the mid-observation time, because of the rapidly changing size of the Earth and its limb. Because of these size changes and the inertial pointing of the spacecraft, these observations obviously suffer from pointing drift that will have to be carefully taken care of at the data analysis stage.
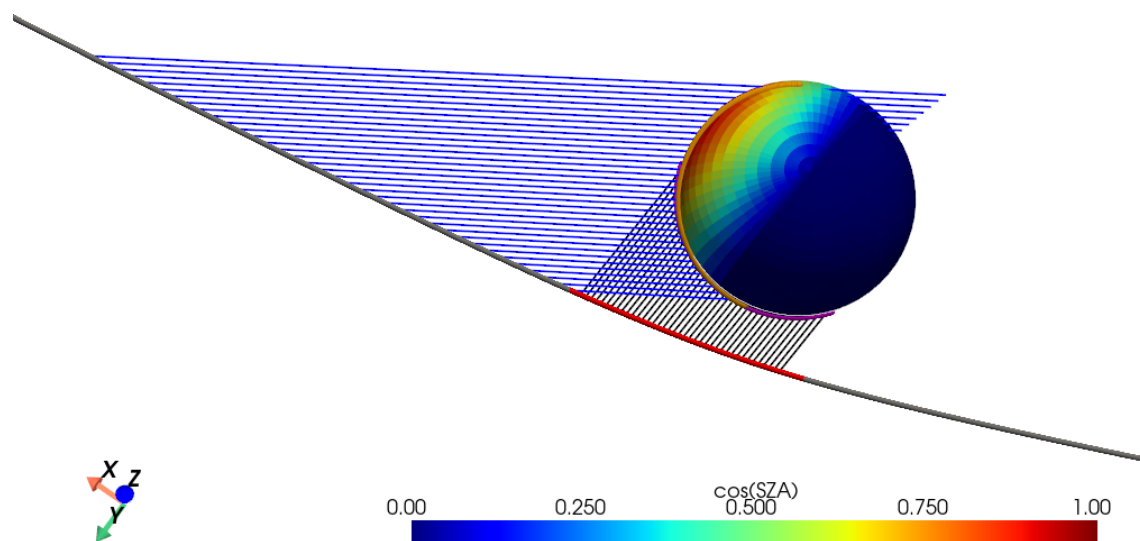
Figure 6. Modeled view of the Moon flyby. Colored facets indicate the cosine of the solar zenith angle (SZA). Dark red corresponds to the sub-solar point and dark blue to the anti-solar point. The observer is positioned above the north pole and the spacecraft trajectory, which is shown as a gray line with red dots for times when SWI FOV intersected the Moon surface during the first observation (ObsID 227) and direction of SWI FOV is shown as black lines. The blue lines represent the SWI boresight direction for the second observation (ObsID 228). The spacecraft flies from right to left (from night-side to day-side) and the velocity vector is following the gray line in that direction. Therefore, from this view angle one can see that the angle between the spacecraft velocity vector and the SWI FOV is close to 90° for the first observation (actually in the range from 110° to 115°) and even larger (approximately 160°) for the second one.

4.4 Later LEGA observations

390   A few hours after the Earth closest approach, a rotation of the spacecraft of 180° around its +X axis enabled SWI to have the Earth and the Moon within the reach of its mechanisms until the end of the LEGA operational phase, i.e., three days after the Earth closest approach. A comprehensive set of calibration and science observations had been prepared to be run over the three days. The observation strategy is detailed hereafter and comprises generic, Moon and Earth observations.
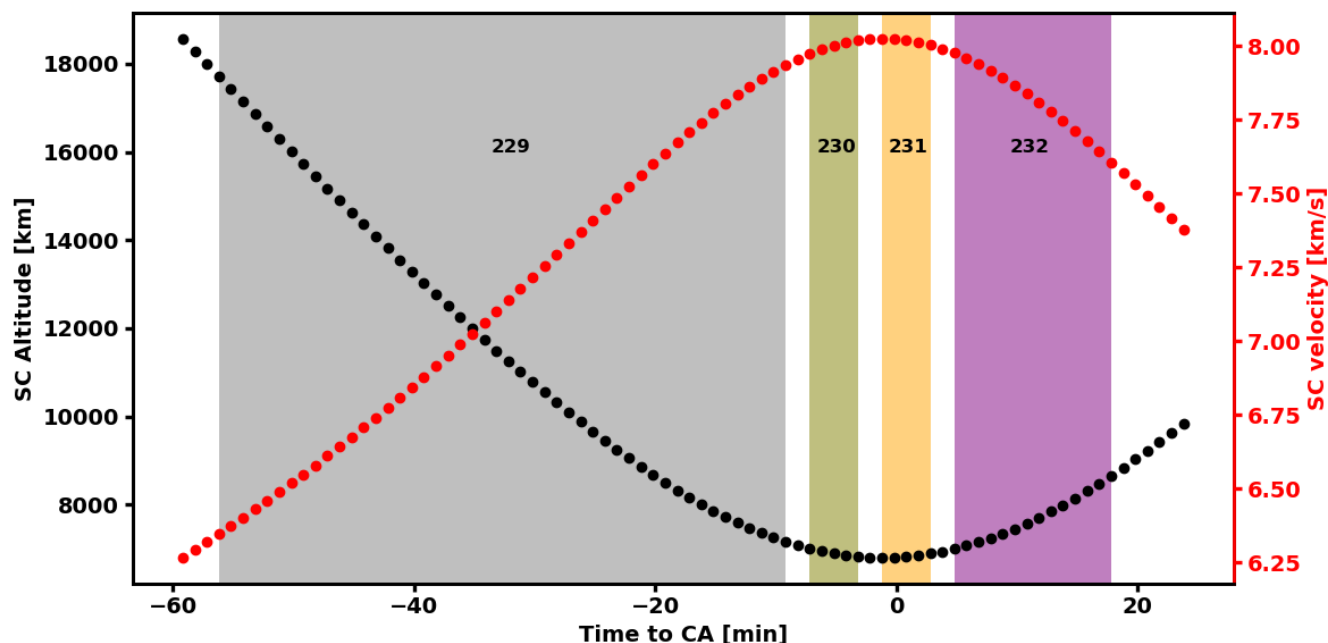
Figure 7. Juice altitude in km (black dots) and relative velocity in km s^{-1} (red dots) around the closest approach during the Earth flyby, on August 20, 2024. The colored areas represent the time windows during which four SWI observations were recorded. The corresponding ObsIDs are labeled.

4.4.1 Generic observations

395   Every operational day started with system temperature measurements (see Table E1 in Appendix E1) to enable a proper radiometric calibration of the data of the same day. The limitation of FLM cycling over the entire mission (Hartogh et al., 2026a) resulted in only using the internal hot load to cali@brate the system temperature measurements and to use those for the relative calibration of other observations using an external hot load at the disk center of the target taken the same day. All these internal/external hot load measurements will serve the purpose of constituting a long-term database for radiometric calibration 400   of SWI data (Jarchow et al., 2026) (this issue).

4.4.2 Moon observations

The goals of the Moon observations were three-fold. We first performed limb stares at the North, South, East and West limbs of the Moon as soon as operations resumed following the Earth gravity assist. The short time delay after the LEGA ensured that the angular size of the Moon was still large enough to consolidate the validation of the instrument pointing offsets, the 405   limb staring mode itself, and to search for a possible water vapor exosphere (Livengood et al., 2015). These observations were recorded on August 21, 2024, from 9:50 to 11:30 UTC, and were supposed to be followed 15 hours later by an AT and a

CT scan across the Moon to measure the beam in both bands. These observations could not be performed because of a safe mode event a few hours earlier, during the execution of ObsID 314 (see next section). After the recovery of the instrument, final Moon observations were carried out in the form of various spectral scans all in nadir (both using the CTS and the ACS, and both in position-switch and frequency-switch) on August 23, 2024, to enable the characterization of the spectral response and constrain baseline standing waves across the full bandwidth. A high-level summary of these observations can be found in Table E2 of Appendix E2.

4.4.3 Earth observations

Numerous Earth observations were made from August 21 to 23, 2024. A high-level summary of these is provided in Table E3 of Appendix E3. In the subsequent discussion, we categorize our approach according to the operational, calibration, or scientific objective. An additional obvious objective was to validate the chosen observation modes.

Using the SWI_2D_MAP_OTF_V1 mode, regular 1D scans were performed either along the AT or CT direction plus/minus a few beams to reach cold space, as shown in Fig. 8 (left)[2]. Also, several 15×15 point maps were planned on August 22 (see Fig. 8 right), with 12 different tunings to cover a variety of lines. Only the last 8 maps were actually performed, after the Mission Operation Center (MOC) was able to restart the instrument's operations timeline following the safe mode triggered by ObsID 314. The goal of these maps was to characterize the beam pattern and verify the pointing accuracy. Examples of these observations are provided as video supplements with the following DOIs: 10.5446/72321, 10.5446/72322, and 10.5446/72325, for ObsID 242, 243, and 373, respectively. This inflight calibration of the antenna pointing and beam characterization is presented in Moreno et al. (2026) (this issue). Additional 1D scans were performed along the equator and along the central meridian. Here, we aimed at validating our commanding for proper tilting of 2D maps in order to align them with the rotation axis of a planet. In practice, the map point coordinates (and consequently the map point AT/CT steps) are rotated by the North Pole angle, which is obtained from the SPICE kernels. This planning feature will be important especially when mapping Jupiter, to align the maps with the rotation axis of the planet and therefore facilitate the planet rotation correction on the spectra of each map point.

Multiple limb stares and limbs scans were performed either with position- or frequency-switching, with the double objective of consolidating the knowledge of the instrument pointing (with respect to the Juice nadir direction) and to confirm several tunings crucial for the Science Phase. To make sure a minimum of useful data would be acquired, Earth-specific tunings with strong O_3 and O_2 lines were also selected among the various one planned in these observations. Two examples of such observations are in Fig. 9 and two others are provided as video supplements with the following DOIs: 10.5446/72323 and 10.5446/72324, for ObsID 257 and 282, respectively.

To further validate the variety of spectral tunings that will later be used during the Science Phase, we scheduled a number of spectral scans either with the CTS or the ACS, both, in position- and frequency-switching mode. In total, we tested 75 selected tunings in each spectral band. These spectral scans are presented in Jarchow et al. (2026) (this issue). The pointing geometry of

---

[2]The planet rendering in Figs. 8 and 9 are made with the help of PlanetMapper python package (King and Fletcher, 2023), available at https://github.com/ortk95/planetmapper.
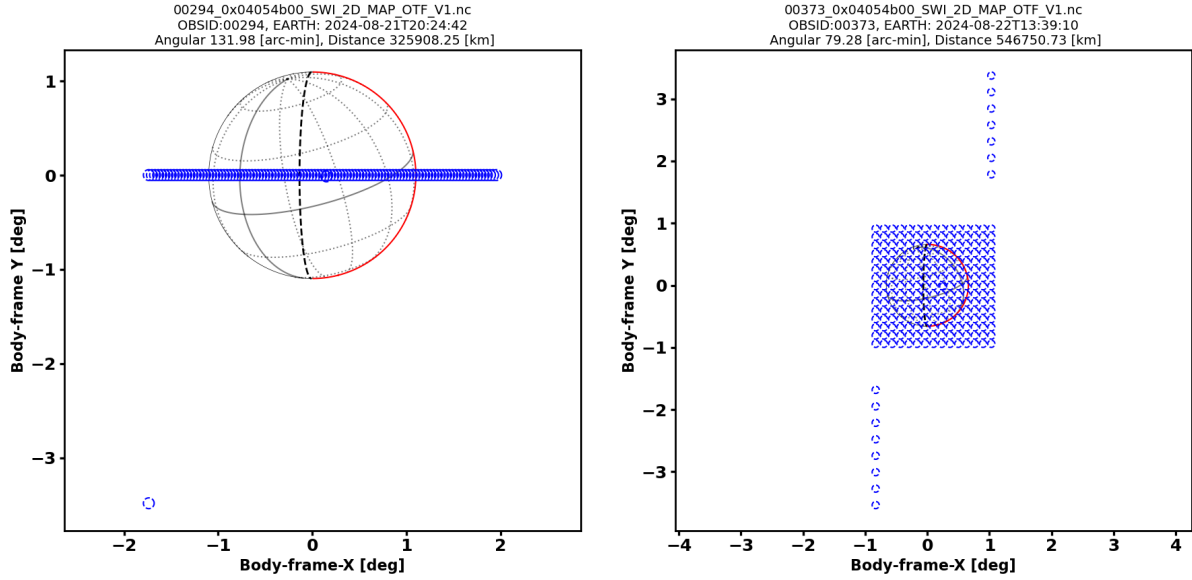
Figure 8. Geometry of the Earth for (Left) the AT scan performed on August 21, 2024, and (Right) one of the 2D OTF maps performed on August 22, 2024, during the LEGA phase. The Earth is represented by the gray circle, with its equator also shown with a gray line. Pointed positions depicted by the blue dashed circles include ON source integrations, the OFF integration (the furthest to the bottom left), and the "external" hotload calibration (slightly right to the disk center). The South Pole is at the top. The first observation served to validate the SWI_2D_MAP_OTF_V1 mode used with a single row. Another observation that used a single column was also successful.

the different spectral scans include nadir and various limb staring positions (see Table E3). Some of the planned spectral scans
440 were eventually not executed because of the safe mode caused by ObsID 314.

5   Conclusions

This paper details the operational, and strategic plan of Juice's SWI instrument during the LEGA mission phase. We also bring into forefront the inherent complexity of this submillimetre mini-telescope, which necessitated extensive validation campaigns and calibration activities. In order to reach the SWI science goals, 31 distinct observation modes were designed, each with its
445 own calibration approach. Currently, 27 of the 31 modes have been validated for operational use, enabling robust scientific observations in the subsequent Science Phase. In the context of SWI operations and planning, our future efforts will focus on validating and refining these modes in the subsequent Earth flybys, EGA #2 and EGA #3, which scheduled as part of Juice tour on its way to Jupiter.

The LEGA operations of SWI have produced a wealth of data, with 166 successful observations, which have been partly
450 explored and analyzed (Jarchow et al., 2026; Moreno et al., 2026) (this issue). It should be noted that the power and telemetry
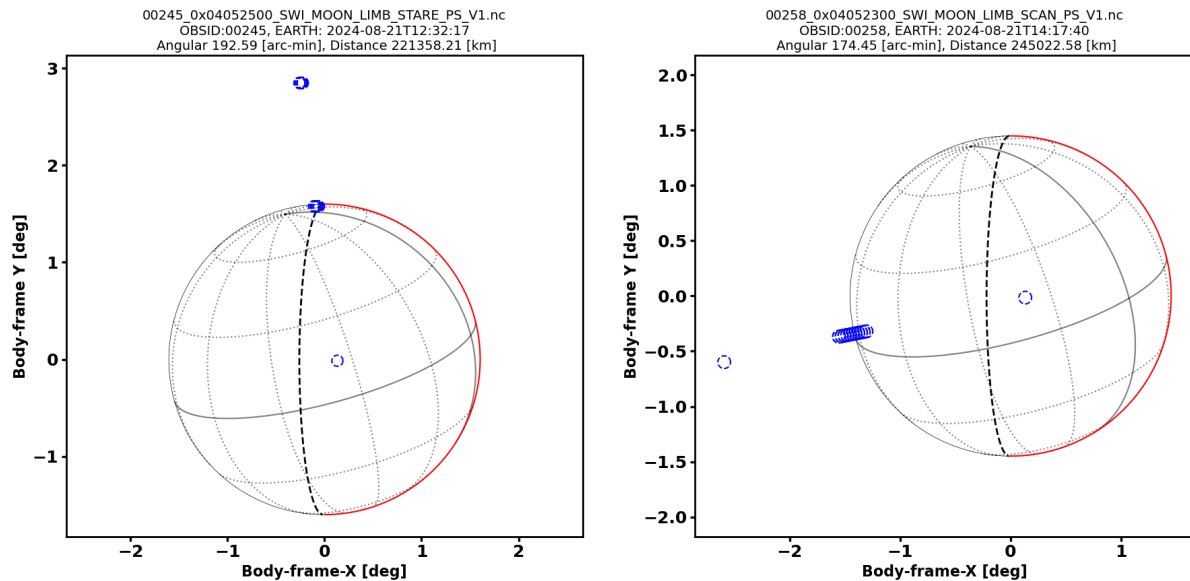
Figure 9. Geometry of the Earth during (Left) the North Pole limb stare and (Right) the equatorial nightside limb scan, both performed on August 21, 2024, during the LEGA phase. Same layout as Fig. 8. These observations served to validate the SWI_MOON_LIMB_STARE_-PS_V1 and SWI_MOON_LIMB_SCAN_PS_V1 modes.

budgets of the SWI were monitored during the entire LEGA activities and were found to conform with predictions. The data acquired during the LEGA will serve to set the foundations of the future Earth Gravity Assists, namely EGA #2 on 28 September 2026 and EGA #3 on 17 January 2029. The instrument highest priorities for EGA #2 and #3 will undoubtedly include the consolidation of the knowledge of uncertainties of the two axes of the pointing mechanism, both absolute and
455 relative. Another goal will be to consolidate the flyby operational strategy, in view of the future Europa, Ganymede and Callisto flybys. A strategy broadly similar to that applied during the LEGA, with AT/CT scans, limb stare/scans, spectral scans, and 2D OTF maps, may thus apply for these EGAs.

Appendix A: Calibration modes

- **SWI_TSYS_CTS_V1**: This mode consists of a spectral scan to measure the system temperature spectra of the 2 bands with the CTS 1 & 2 by observing the hot load and cold sky. Integration time on the CTS is 2 seconds. A single execution can cover up to 15 tunings. The pointing of the spacecraft can be any and the instrument does not use its pointing mechanism.

- **SWI_TSYS_ACS_CCH_V1**: This mode is similar to SWI_TSYS_CTS_V1, but using the ACS & CCH 1 & 2. Integration time on ACS is 1 second. A single execution can cover up to 15 tunings. An initial version this mode, named **SWI_TSYS_ACS_CCH** is no longer used and will be removed from the DPU in a future PCW.

- **SWI_TSYS_ACS_V1**: This mode is similar to SWI_TSYS_ACS_CCH_V1, but CCH 1 & 2 are switched off. A single execution can cover up to 16 tunings.

- **SWI_TSYS_CCH_V1**: This mode is similar to SWI_TSYS_ACS_CCH_V1, but ACS 1 & 2 are switched off. A single execution can cover up to 16 tunings.

- **SWI_ALLAN_CTS_FS**: Allan variance characterization of the CTS 1 & 2 by integrating on the cold sky. Integration time is 1.5 s and the calibration method is frequency-switch. The pointing of the spacecraft can be any and the instrument does not use its pointing mechanism.

- **SWI_ALLAN_ACS_FS**: This mode is similar to SWI_ALLAN_CTS_FS, but using the ACS 1 & 2. Integration time is 1 s.

- **SWI_ALLAN_TOTAL_CTS**: Total power Allan variance characterization of the CTS 1 & 2 by integrating on the cold sky. Integration time is 1.5 s. The pointing of the spacecraft can be any and the instrument does not use its pointing mechanism.

- **SWI_ALLAN_TOTAL_ACS**: This mode is similar to SWI_ALLAN_TOTAL_CTS, but using the ACS 1 & 2. Integration time is 1 s.

- **SWI_ALLAN_TOTAL_CCH**: This mode is similar to SWI_ALLAN_TOTAL_CTS, but using the CCH 1 & 2. Integration time is 1 s.

It should be noted that all integration times are only given for typical use cases, but are parameters when invoking a mode and can thus be tuned to the desired value.

Appendix B: Science observation modes

- **SWI_NADIR_STARE_PS_V1**: Staring observations in the nadir position of the instrument (the spacecraft pointing can either be nadir or limb) to investigate atmospheric composition and temperature of Jupiter and the Galilean moons (see Fig. B1 left). This mode is nominally meant for deep integrations and requires numerous repetitions. Nominally, two CTS spectra are recorded for 60 seconds over 10000 channels using a position-switch calibration
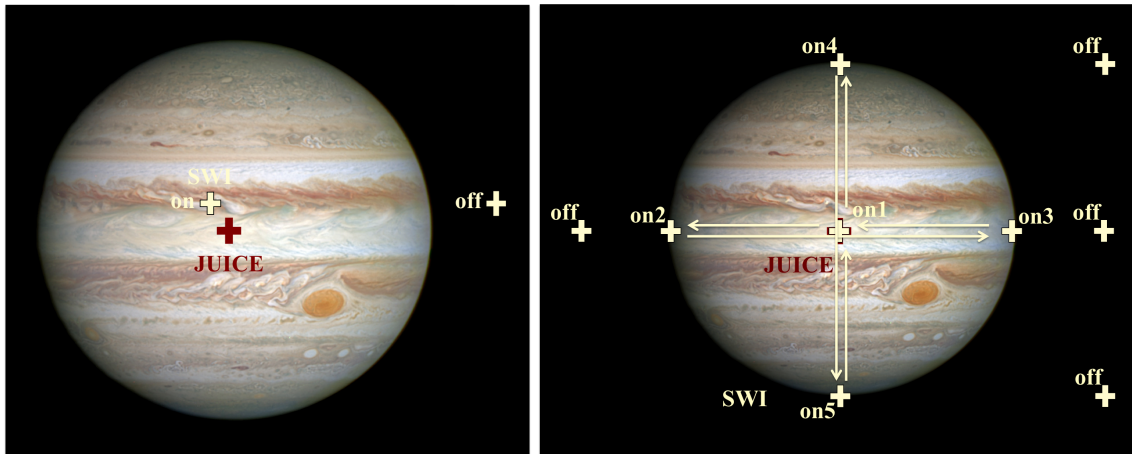
Figure B1. (Left) SWI_NADIR_STARE_* or SWI_MOON_NADIR_STARE* (and also SWI_SPECTRAL_SCAN_ACS_* and SWI_-SPECTRAL_SCAN_CTS_*) and (Right) SWI_5POINT_CROSS_* mode geometries. In frequency-switch, there is no need for OFF position pointing.

method. An initial version this mode, named **SWI_NADIR_STARE_PS** is no longer used and will be removed from the DPU in a future PCW.

- **SWI_NADIR_STARE_FS_V1**: Same as SWI_NADIR_STARE_PS_V1, except a frequency-switch calibration mode is used instead of position-switch. It enables spending ∼100% of the integration time on-source. If the purity of the spectral band is good enough, there is an option to pre-compute ON−OFF for the CTS before downlink.

- **SWI_5POINT_CROSS_PS_V1**: Rough raster mapping using a 5-point cross to investigation of the Jovian and Galilean moon atmospheric composition, and Galilean surface properties (see Fig. B1 right). The stepsize is such that the opposite ends of the cross are separated by the size of the target in the given direction. For Jupiter, two CTS spectra are recorded for 60 seconds over 10000 channels. For moon monitoring, two CTS spectra are recorded for 30 seconds over 210 channels. For both cases, and in parallel, two CCH measurements are recorded every 1-2 seconds. A position-switch calibration method is used.

- **SWI_5POINT_CROSS_FS_V1**: Same as SWI_5POINT_CROSS_PS_V1, except a frequency-switch calibration mode is used instead of position-switch. It enables spending ∼100% of the integration time on-source. If the purity of the spectral band is good enough, there is an option to pre-compute ON−OFF for the CTS before downlink. Frequency-switch calibration method for CTS data.

- **SWI_2D_MAP_PS_V1**: This is a multi-purpose mode that can be used on any science target for any 2D mapping (see Fig. B2), and can be customized into meridional or zonal rasters. This mode can also be used for pointing calibration purposes. The number of rows and columns and the stepsize of the raster map is adaptable to the target angular size. For Jupiter, this mode is used for the investigation of the global and regional stratospheric compo-
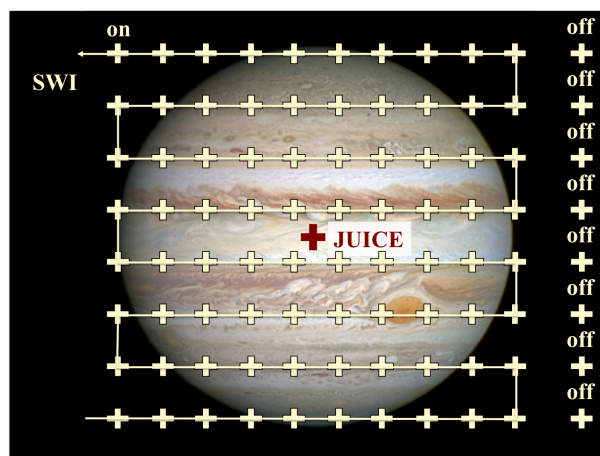
Figure B2. Various SWI_2D_MAP_* mode geometries. Steps on the figures are only indicative and actually depend on science goal. This generic 2D map can be used for pointing calibration, Jupiter mapping or moon monitoring. IT can be customized to a meridional raster or to a zonal raster. In frequency-switch, there is no need for OFF position pointing. In the On-the-fly (OTF) mode, the OFF position is observed only once per row.

sition and temperature of Jupiter, and pointing calibration. For 2D maps, meridional scans and zonal scans, two CTS spectra are recorded for 60 seconds over 10000 channels. For moon monitoring, it is used to investigate the spatial distribution of Galilean moons atmospheric species (+ monitoring), and calibration. Two CTS spectra are recorded for 60 seconds over 210 channels. During flybys, it is used to map Galilean Moon surface properties and atmospheric composition, temperature, and winds. Two CTS spectra are recorded for 30 seconds over 210 channels. During GCO, it is used to (1) Investigate Ganymede's atmospheric composition, temperature, and winds, and surface properties by scanning from limb to limb with the along-track mechanism across the ground-track using the antenna mechanism ($\pm 72°$) and two CTS spectra are recorded for 10 seconds over 130 channels, (2) to perform tomographic investigation of Ganymede's atmospheric and surface composition, temperature, and winds by scanning along-track from -30km to $+30$km of the nadir axis with 9 steps, using the rocker mechanism ($\pm 4.3°$), and with 1.5 sec integration time for two CTS spectra over 130 channels. In all cases, two CCH measurements are recorded every 0.375-1 second. During GCO, this implies that two CCH measurements are separated by 1/2 beam at 1200 GHz. This mode uses the position-switch calibration method (the OFF position is observed after each ON of the map is observed).

- **SWI_2D_MAP_FS_V1**: Same as SWI_2D_MAP_PS_V1, except a frequency-switch calibration mode is used instead of position-switch.

- **SWI_2D_MAP_OTF_V1**: Same as SWI_2D_MAP_PS_V1, but using an on-the-fly recording sequence, i.e. the OFF position per map row is only observed once. An initial version this mode, named **SWI_2D_MAP_OTF** is no longer used and will be removed from the DPU in a future PCW.

- **SWI_2D_MAP_OTF_CCH_V1**: Same as SWI_2D_MAP_OTF_V1, but this mode uses the CCH only.

- **SWI_SPECTRAL_SCAN_ACS_PS_V1**: This mode is used for the investigation of the atmospheric composition of Jupiter and the Galilean moons using a fixed pointed position on the target, in the same way as SWI_NADIR_-STARE_PS_V1 (see. Fig. B1 left). The whole frequency range available to SWI is scanned. This mode is nominally meant for deep integrations and requires numerous repetitions. Two ACS spectra are recorded for 60 seconds over 1024 channels. Position-switch calibration method. A single execution can cover up to 16 tunings.

- **SWI_SPECTRAL_SCAN_ACS_FS_V1**: Same as SWI_SPECTRAL_SCAN_ACS_PS_V1, except a frequency-switch calibration mode is used instead of position-switch. A single execution can cover up to 11 tunings.

- **SWI_SPECTRAL_SCAN_CTS_PS_V1**: Same as SWI_SPECTRAL_SCAN_ACS_PS_V1, except the CTS are used instead of the ACS. Two CTS spectra are recorded for 60 seconds over 10000 channels using a position-switch calibration method. A single execution can cover up to 13 tunings.

- **SWI_SPECTRAL_SCAN_CTS_FS_V1**: Same as SWI_SPECTRAL_SCAN_CTS_PS_V1, except a frequency-switch calibration mode is used instead of position-switch. A single execution can cover up to 9 tunings.

- **SWI_JUP_LIMB_STARE_PS_V1**: This mode is especially designed for the investigation of Jupiter's stratospheric dynamics, composition and temperature by targeting one (or more) molecular line(s) at the planetary limb. The pointed latitude can be chosen. The retrieval of vertical profiles require a very high signal-to-noise ratio ($\sim$100) and a very high spectral resolution (100 kHz). A coarser spectral resolution (i.e., 500 kHz) is sufficient for detections. This mode is nominally meant for deep integrations and implies numerous repetitions. A short $\sim$10-point across-limb scan of the continuum emission is performed with the CCH to derive a posteriori the instrument pointing and enabling accurate planet-rotation compensation (to get the zonal wind speeds), followed by two CTS spectra recorded for 60 seconds over 10000 channels (and two CCH measurements recorded every 2 seconds). The position-switch calibration method is used. This mode is presented in Fig. B3 left.

- **SWI_JUP_LIMB_STARE_FS_V1**: Same as SWI_JUP_LIMB_STARE_PS_V1, except a frequency-switch calibration mode is used instead of position-switch.

- **SWI_JUP_LIMB_RASTER_PS_V1**: This mode combine several limb stares from SWI_JUP_LIMB_STARE_V1 into a full series to cover a set of latitudes in a single execution. This mode is presented in Fig. B3 right).

- **SWI_JUP_LIMB_RASTER_FS_V1**: Same as SWI_JUP_LIMB_RASTER_PS_V1, except a frequency-switch calibration mode is used instead of position-switch.

- **SWI_MOON_LIMB_STARE_PS_V1**: This mode is used for the investigation of Galilean Moons atmospheric composition, temperature, and winds, by pointing to a fixed position on the limb of the target (Fig. B4 left). The pointed latitude and altitude can be chosen. *Flyby:* Two CTS spectra are recorded for 30 sec over 210 channels. *GCO:* Two CTS spectra are recorded for 30 sec over 130 channels and a different altitude (5, 10, 20, 40, and 50 km) is scanned every orbit. this mode uses the position-switch calibration method.
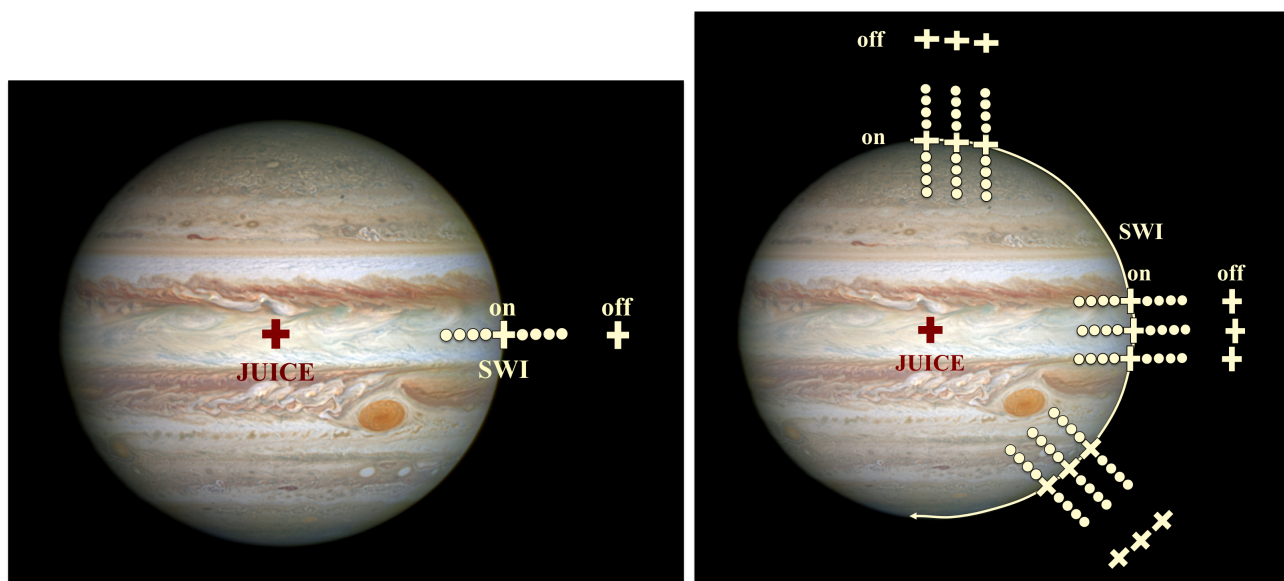
Figure B3. (Left) SWI_JUP_LIMB_STARE_* mode geometry. (Right) SWI_JUP_LIMB_RASTER_* mode geometry. Each point in these modes includes a small across-limb scan to retrieved a posteriori the precise pointing of SWI. The number of points in the across-limb scan is ∼10, but integration times (∼0.375 s) and therefore overheads should be short. In frequency-switch, there is no need for OFF position pointing.
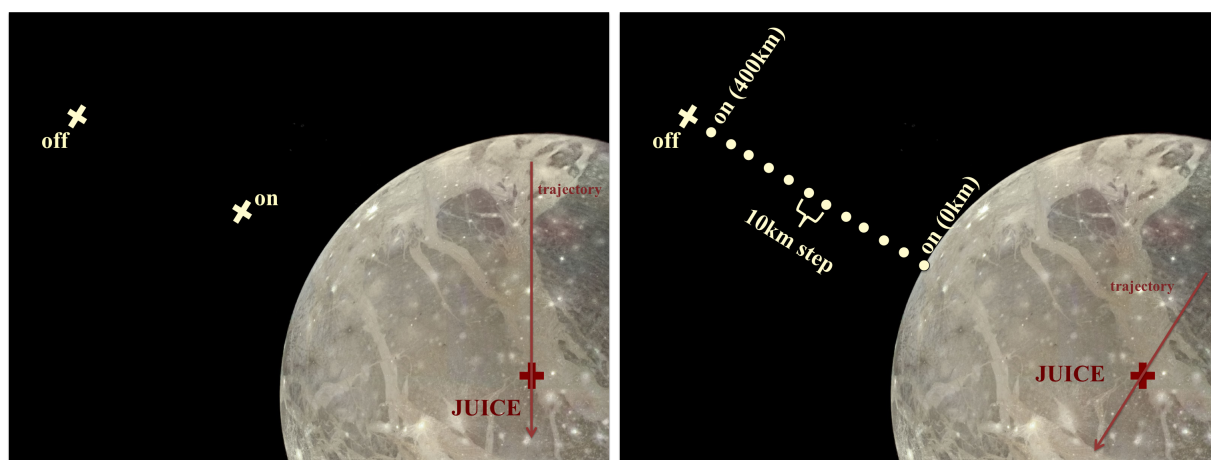
Figure B4. (Left) SWI_MOON_LIMB_STARE_* mode geometry. (Right) SWI_MOON_LIMB_SCAN_* mode geometry. In frequency-switch, there is no need for OFF position pointing.

- **SWI_MOON_LIMB_STARE_FS_V1**: Same as SWI_MOON_LIMB_STARE_PS_V1, except a frequency-switch calibration mode is used instead of position-switch.

- **SWI_MOON_LIMB_SCAN_PS_V1**: This mode serves to investigate the Galilean Moons atmospheric composition, temperature, and winds. *Flyby:* The atmospheric limb is rapidly scanned at a chosen latitude to achieve 5 km vertical resolution (Fig. B4 right). Two CTS spectra are recorded for 1.5 sec over 210 channels (16 bits coding). *GCO:* The atmospheric limb is scanned up and down rapidly with 10 km altitude steps and with 1.5 sec integration time for two CTS spectra over 130 channels. This mode uses a position-switch calibration method.

- **SWI_MOON_LIMB_SCAN_FS_V1**: Same as SWI_MOON_LIMB_SCAN_PS_V1, except a frequency-switch calibration mode is used instead of position-switch.

- **SWI_MOON_NADIR_STARE_PS_V1**: This mode can be invoked for the investigation of Galilean Moons atmospheric composition, temperature, and winds, and surface properties. This mode can also be used to characterize surface polarization by pointing 45° off-nadir, after rotating the S/C by 90° around its nadir axis. It can also serve for solar occultation experiments to observe a weak molecular line in the atmosphere of Jupiter, a Galilean Moon, or the Europa torus. It uses the same concept as SWI_NADIR_STARE_PS_V1, except the CCH are also used. During flyby, two CTS spectra are recorded for 30 seconds over 210 channels. During GCO, two CTS spectra are recorded for 10 seconds over 130 channels. In both cases, two CCH measurements are recorded every 0.5-1 second, so that they are separated by maximum 1/2 beam at 1200 GHz. During solar occultations, two CTS spectra are recorded for 60 seconds over 10000 channels, and two CCH measurements are recorded every 2 seconds. This mode uses the position-switch calibration method.

- **SWI_MOON_NADIR_STARE_FS_V1**: Same as SWI_MOON_NADIR_STARE_PS_V1, except a frequency-switch calibration mode is used instead of position-switch.

Similarly to the calibration modes (see Appendix A), all integration times are only given for typical use cases, but are parameters when invoking a mode and can thus be tuned to the desired value.

Appendix C: Moon flyby

The two Moon observations that SWI recorded during the Moon-Gravity-Assist are detailed in Table C1.

Table C1: Observations during the Moon flyby.

Date	ObsID	Obs. mode	LO setup	Comment	Status
2024-08-19T20:42:14	227	SWI_2D_MAP_OTF_V1	H_2O	Sub-spacecraft track	completed
2024-08-19T21:26:27	228	SWI_2D_MAP_OTF_V1	H_2O	Backward look track	completed

585

Appendix D: Earth flyby

The four Earth observations performed by SWI during the Earth-Gravity-Assist are presented in Table D1.

Table D1: Observations during the Earth flyby.

Date	ObsID	Obs. mode	LO setup	Comment	Status
2024-08-20T21:00:11	229	SWI_2D_MAP_OTF_V1	H_2O	Sub-spacecraft track	completed
2024-08-20T21:49:11	230	SWI_MOON_LIMB_SCAN_PS_V1	H_2O, HDO		completed
2024-08-20T21:55:11	231	SWI_MOON_LIMB_STARE_PS_V1	H_2O, $H_2^{17}O$, $H_2^{18}O$		completed
2024-08-20T22:01:11	232	SWI_2D_MAP_OTF_V1	H_2O	Backward look track	completed

590 ## Appendix E: Later LEGA observations

E1 Generic observations

The radiometric calibration observations recorded after the Earth-Gravity-Assist are detailed in Table E1.

Table E1: Radiometric calibration observations for system temperature derivation, taken after the Earth gravity assist. Subsequent to the safe mode triggered by ObsID 314 (see Table E2), ObsIDs 322 was not executed.

Date	ObsID	Obs. mode	LO setup	Status
2024-08-21T11:30:12	237	SWI_TSYS_CTS_V1	15 tunings	completed
2024-08-21T11:36:12	238	SWI_TSYS_CTS_V1	15 tunings	completed
2024-08-21T11:42:12	239	SWI_TSYS_CTS_V1	15 tunings	completed
2024-08-21T11:48:12	240	SWI_TSYS_CTS_V1	15 tunings	completed
2024-08-21T11:54:12	241	SWI_TSYS_CTS_V1	15 tunings	completed
2024-08-22T00:18	322	SWI_TSYS_CTS_V1	15 tunings	not executed

Date	ObsID	Obs. mode	LO setup	Status
2024-08-23T06:30:12	381	SWI_TSYS_CTS_V1	15 tunings	completed
2024-08-23T06:36:12	382	SWI_TSYS_CTS_V1	15 tunings	completed
2024-08-23T06:42:12	383	SWI_TSYS_CTS_V1	15 tunings	completed
2024-08-23T06:48:12	384	SWI_TSYS_CTS_V1	15 tunings	completed
2024-08-23T06:54:12	385	SWI_TSYS_CTS_V1	15 tunings	completed
2024-08-23T12:30:12	414	SWI_TSYS_ACS_CCH_V1	17 tunings	completed
2024-08-23T12:36:11	415	SWI_TSYS_ACS_CCH_V1	17 tunings	completed
2024-08-23T12:42:11	416	SWI_TSYS_ACS_CCH_V1	17 tunings	completed
2024-08-23T12:48:11	417	SWI_TSYS_ACS_CCH_V1	17 tunings	completed

595

E2 Moon observations

The Moon observations performed after the the Earth-Gravity-Assist are summarized in Table E2.

Table E2: Observations of the Moon after the Earth gravity assist. Subsequent to the safe mode triggered by ObsID 314, ObsIDs 323-334 were not executed. ObsIDs 412 and 413 were voluntarily skipped as a precaution because they had similar parameters as ObsID 314 and were considered a safe mode risk at the time. Eq. and b stand for the Equator and the beam size in the 600 GHz band, respectively.

Date	ObsID	Obs. mode	LO setup	Comment	Status
2024-08-21T09:50:12	233	SWI_MOON_LIMB_STARE_PS_V1	H_2O	Dawn, Eq.	completed
2024-08-21T10:15:12	234	SWI_MOON_LIMB_STARE_PS_V1	H_2O	Dusk, Eq.	completed
2024-08-21T10:40:12	235	SWI_MOON_LIMB_STARE_PS_V1	H_2O	South Pole	completed
2024-08-21T11:05:12	236	SWI_MOON_LIMB_STARE_PS_V1	H_2O	North Pole	completed
2024-08-22T00:24	323	SWI_2D_MAP_OTF_V1	H_2O	AT scan $\pm 4b$	not executed
2024-08-22T00:27	324	SWI_2D_MAP_OTF_V1	H_2O	CT scan $\pm 4b$	not executed
2024-08-22T00:30	325	SWI_MOON_NADIR_STARE_PS_V1	H_2O	Moon center	not executed
2024-08-22T00:34	326	SWI_MOON_LIMB_STARE_PS_V1	H_2O	Dawn, Eq.	not executed
2024-08-22T00:38	327	SWI_MOON_LIMB_STARE_PS_V1	H_2O	Dusk, Eq.	not executed
2024-08-22T00:42	328	SWI_MOON_LIMB_STARE_PS_V1	H_2O	South Pole	not executed
2024-08-22T00:46	329	SWI_MOON_LIMB_STARE_PS_V1	H_2O	North Pole	not executed
2024-08-22T00:50	330	SWI_MOON_NADIR_STARE_FS_V1	H_2O	Moon center	not executed
2024-08-22T01:10	331	SWI_MOON_LIMB_STARE_FS_V1	H_2O	Dawn, Eq.	not executed

Date	ObsID	Obs. mode	LO setup	Comment	Status
2024-08-22T01:35	332	SWI_MOON_LIMB_STARE_FS_V1	H_2O	Dusk, Eq.	not executed
2024-08-22T02:00	333	SWI_MOON_LIMB_STARE_FS_V1	H_2O	South Pole	not executed
2024-08-22T02:25	334	SWI_MOON_LIMB_STARE_FS_V1	H_2O	North Pole	not executed
2024-08-23T09:42:11	400	SWI_SPECTRAL_SCAN_CTS_PS_V1	11 tunings	Moon center	completed
2024-08-23T09:53:11	401	SWI_SPECTRAL_SCAN_CTS_PS_V1	11 tunings	Moon center	completed
2024-08-23T10:04:11	402	SWI_SPECTRAL_SCAN_CTS_PS_V1	11 tunings	Moon center	completed
2024-08-23T10:15:11	403	SWI_SPECTRAL_SCAN_CTS_PS_V1	11 tunings	Moon center	completed
2024-08-23T10:26:11	404	SWI_SPECTRAL_SCAN_CTS_PS_V1	11 tunings	Moon center	completed
2024-08-23T10:37:11	405	SWI_SPECTRAL_SCAN_CTS_PS_V1	11 tunings	Moon center	completed
2024-08-23T10:48:11	406	SWI_SPECTRAL_SCAN_CTS_FS_V1	8 tunings	Moon center	completed
2024-08-23T11:00:11	407	SWI_SPECTRAL_SCAN_CTS_FS_V1	8 tunings	Moon center	completed
2024-08-23T11:12:11	408	SWI_SPECTRAL_SCAN_CTS_FS_V1	8 tunings	Moon center	completed
2024-08-23T11:24:11	409	SWI_SPECTRAL_SCAN_CTS_FS_V1	8 tunings	Moon center	completed
2024-08-23T11:36:11	410	SWI_SPECTRAL_SCAN_CTS_FS_V1	8 tunings	Moon center	completed
2024-08-23T11:48:11	411	SWI_SPECTRAL_SCAN_CTS_FS_V1	8 tunings	Moon center	completed
2024-08-23T12:00:11	412	SWI_SPECTRAL_SCAN_CTS_FS_V1	8 tunings	Moon center	not executed
2024-08-23T12:12:11	413	SWI_SPECTRAL_SCAN_CTS_FS_V1	8 tunings	Moon center	not executed
2024-08-23T15:48:11	429	SWI_SPECTRAL_SCAN_ACS_PS_V1	13 tunings	Moon center	completed
2024-08-23T16:04:11	430	SWI_SPECTRAL_SCAN_ACS_PS_V1	13 tunings	Moon center	completed
2024-08-23T16:20:11	431	SWI_SPECTRAL_SCAN_ACS_PS_V1	13 tunings	Moon center	completed
2024-08-23T16:36:11	432	SWI_SPECTRAL_SCAN_ACS_PS_V1	13 tunings	Moon center	completed
2024-08-23T16:52:11	433	SWI_SPECTRAL_SCAN_ACS_PS_V1	13 tunings	Moon center	completed
2024-08-23T17:08:11	434	SWI_SPECTRAL_SCAN_ACS_FS_V1	10 tunings	Moon center	completed
2024-08-23T17:22:11	435	SWI_SPECTRAL_SCAN_ACS_FS_V1	10 tunings	Moon center	completed
2024-08-23T17:36:11	436	SWI_SPECTRAL_SCAN_ACS_FS_V1	10 tunings	Moon center	completed
2024-08-23T17:50:11	437	SWI_SPECTRAL_SCAN_ACS_FS_V1	10 tunings	Moon center	completed
2024-08-23T18:04:11	438	SWI_SPECTRAL_SCAN_ACS_FS_V1	10 tunings	Moon center	completed
2024-08-23T18:18:11	439	SWI_SPECTRAL_SCAN_ACS_FS_V1	10 tunings	Moon center	completed

600

E3 Earth observations

The various Earth observations performed after the the Earth-Gravity-Assist are summarized in Table E3.

Table E3: Observations of the Earth after the Earth gravity assist. Subsequent to the safe mode triggered by ObsID 314 (see Table E2), Earth observations corresponding to ObsIDs 315-372 were not executed. Eq., CM and b stand for the Equator, the Central Meridian and the beam size in the 600 GHz band, respectively.

Date	ObsID	Obs. mode	LO setup	Comment	Status
2024-08-21T12:00:12	242	SWI_2D_MAP_OTF_V1	H_2O	AT scan $\pm10b$	completed
2024-08-21T12:07:12	243	SWI_2D_MAP_OTF_V1	H_2O	CT scan $\pm10b$	completed
2024-08-21T12:14:12	244	SWI_NADIR_STARE_PS_V1	H_2O	Nadir	completed
2024-08-21T12:28:12	245	SWI_MOON_LIMB_STARE_PS_V1	H_2O	73S	completed
2024-08-21T12:36:12	246	SWI_MOON_LIMB_STARE_PS_V1	H_2O	50S 90W	completed
2024-08-21T12:44:12	247	SWI_MOON_LIMB_STARE_PS_V1	H_2O	50S 90E	completed
2024-08-21T12:52:12	248	SWI_MOON_LIMB_STARE_PS_V1	H_2O	20S 90W	completed
2024-08-21T13:00:12	249	SWI_MOON_LIMB_STARE_PS_V1	H_2O	20S 90E	completed
2024-08-21T13:08:12	250	SWI_MOON_LIMB_STARE_PS_V1	H_2O	Eq 90W	completed
2024-08-21T13:16:12	251	SWI_MOON_LIMB_STARE_PS_V1	H_2O	Eq 90E	completed
2024-08-21T13:24:12	252	SWI_MOON_LIMB_STARE_PS_V1	H_2O	20N 90W	completed
2024-08-21T13:32:12	253	SWI_MOON_LIMB_STARE_PS_V1	H_2O	20N 90E	completed
2024-08-21T13:40:12	254	SWI_MOON_LIMB_STARE_PS_V1	H_2O	50N 90W	completed
2024-08-21T13:48:12	255	SWI_MOON_LIMB_STARE_PS_V1	H_2O	50N 90E	completed
2024-08-21T13:56:12	256	SWI_MOON_LIMB_STARE_PS_V1	H_2O	73N	completed
2024-08-21T14:04:12	257	SWI_MOON_LIMB_SCAN_PS_V1	H_2O	Dayside Eq.	completed
2024-08-21T14:13:12	258	SWI_MOON_LIMB_SCAN_PS_V1	H_2O	Nightside Eq.	completed
2024-08-21T14:22:12	259	SWI_2D_MAP_OTF_V1	H_2O	Eq. $\pm4b$	completed
2024-08-21T14:42:12	260	SWI_2D_MAP_OTF_V1	H_2O	CM $\pm4b$	completed
2024-08-21T15:02:12	261	SWI_SPECTRAL_SCAN_CTS_PS_V1	11 tunings	Day Eq. limb	completed
2024-08-21T15:10:12	262	SWI_SPECTRAL_SCAN_CTS_PS_V1	11 tunings	Day Eq. limb	completed
2024-08-21T15:18:12	263	SWI_SPECTRAL_SCAN_CTS_PS_V1	11 tunings	Day Eq. limb	completed
2024-08-21T15:26:12	264	SWI_SPECTRAL_SCAN_CTS_PS_V1	11 tunings	Day Eq. limb	completed
2024-08-21T15:34:12	265	SWI_SPECTRAL_SCAN_CTS_PS_V1	11 tunings	Day Eq. limb	completed
2024-08-21T15:42:12	266	SWI_SPECTRAL_SCAN_CTS_PS_V1	11 tunings	Day Eq. limb	completed
2024-08-21T15:50:12	267	SWI_SPECTRAL_SCAN_CTS_PS_V1	11 tunings	Day Eq. limb	completed
2024-08-21T15:58:12	268	SWI_2D_MAP_OTF_V1	O_3, O_2	AT scan $\pm8b$	completed
2024-08-21T16:05:12	269	SWI_2D_MAP_OTF_V1	O_3, O_2	CT scan $\pm8b$	completed
2024-08-21T16:12:12	270	SWI_NADIR_STARE_PS_V1	O_3, O_2	Nadir	completed

Date	ObsID	Obs. mode	LO setup	Comment	Status
2024-08-21T16:26:12	271	SWI_MOON_LIMB_STARE_PS_V1	O_3, O_2	73S	completed
2024-08-21T16:34:12	272	SWI_MOON_LIMB_STARE_PS_V1	O_3, O_2	50S 90W	completed
2024-08-21T16:42:12	273	SWI_MOON_LIMB_STARE_PS_V1	O_3, O_2	50S 90E	completed
2024-08-21T16:50:12	274	SWI_MOON_LIMB_STARE_PS_V1	O_3, O_2	20S 90W	completed
2024-08-21T16:58:12	275	SWI_MOON_LIMB_STARE_PS_V1	O_3, O_2	20S 90E	completed
2024-08-21T17:06:12	276	SWI_MOON_LIMB_STARE_PS_V1	O_3, O_2	Eq 90W	completed
2024-08-21T17:14:12	277	SWI_MOON_LIMB_STARE_PS_V1	O_3, O_2	Eq 90E	completed
2024-08-21T17:22:12	278	SWI_MOON_LIMB_STARE_PS_V1	O_3, O_2	20N 90W	completed
2024-08-21T17:30:12	279	SWI_MOON_LIMB_STARE_PS_V1	O_3, O_2	20N 90E	completed
2024-08-21T17:38:12	280	SWI_MOON_LIMB_STARE_PS_V1	O_3, O_2	50N 90W	completed
2024-08-21T17:46:12	281	SWI_MOON_LIMB_STARE_PS_V1	O_3, O_2	50N 90E	completed
2024-08-21T17:54:12	282	SWI_MOON_LIMB_STARE_PS_V1	O_3, O_2	73N	completed
2024-08-21T18:03:12	283	SWI_MOON_LIMB_SCAN_PS_V1	O_3, O_2	Dayside Eq.	completed
2024-08-21T18:12:12	284	SWI_MOON_LIMB_SCAN_PS_V1	O_3, O_2	Nightside Eq.	completed
2024-08-21T18:21:12	285	SWI_2D_MAP_OTF_V1	O_3, O_2	Eq. $\pm 4b$	completed
2024-08-21T18:39:12	286	SWI_2D_MAP_OTF_V1	O_3, O_2	CM $\pm 4b$	completed
2024-08-21T18:57:12	287	SWI_SPECTRAL_SCAN_CTS_PS_V1	11 tunings	North pole	completed
2024-08-21T19:09:12	288	SWI_SPECTRAL_SCAN_CTS_PS_V1	11 tunings	North pole	completed
2024-08-21T19:21:12	289	SWI_SPECTRAL_SCAN_CTS_PS_V1	11 tunings	North pole	completed
2024-08-21T19:33:12	290	SWI_SPECTRAL_SCAN_CTS_PS_V1	11 tunings	North pole	completed
2024-08-21T19:45:12	291	SWI_SPECTRAL_SCAN_CTS_PS_V1	11 tunings	North pole	completed
2024-08-21T19:57:12	292	SWI_SPECTRAL_SCAN_CTS_PS_V1	11 tunings	North pole	completed
2024-08-21T20:09:12	293	SWI_SPECTRAL_SCAN_CTS_PS_V1	11 tunings	North pole	completed
2024-08-21T20:21:12	294	SWI_2D_MAP_OTF_V1	HCl, HCN	AT scan $\pm 6b$	completed
2024-08-21T20:27:12	295	SWI_2D_MAP_OTF_V1	HCl, HCN	CT scan $\pm 6b$	completed
2024-08-21T20:33:12	296	SWI_NADIR_STARE_FS_V1	HCl, HCN	Nadir	completed
2024-08-21T20:45:12	297	SWI_MOON_LIMB_STARE_FS_V1	HCl, HCN	73S	completed
2024-08-21T20:51:12	298	SWI_MOON_LIMB_STARE_FS_V1	HCl, HCN	50S 90W	completed
2024-08-21T20:57:12	299	SWI_MOON_LIMB_STARE_FS_V1	HCl, HCN	50S 90E	completed
2024-08-21T21:03:12	300	SWI_MOON_LIMB_STARE_FS_V1	HCl, HCN	20S 90W	completed
2024-08-21T21:09:12	301	SWI_MOON_LIMB_STARE_FS_V1	HCl, HCN	20S 90E	completed
2024-08-21T21:15:12	302	SWI_MOON_LIMB_STARE_FS_V1	HCl, HCN	Eq 90W	completed

Date	ObsID	Obs. mode	LO setup	Comment	Status
2024-08-21T21:21:12	303	SWI_MOON_LIMB_STARE_FS_V1	HCl, HCN	Eq 90E	completed
2024-08-21T21:27:12	304	SWI_MOON_LIMB_STARE_FS_V1	HCl, HCN	20N 90W	completed
2024-08-21T21:33:12	305	SWI_MOON_LIMB_STARE_FS_V1	HCl, HCN	20N 90E	completed
2024-08-21T21:39:12	306	SWI_MOON_LIMB_STARE_FS_V1	HCl, HCN	50N 90W	completed
2024-08-21T21:45:12	307	SWI_MOON_LIMB_STARE_FS_V1	HCl, HCN	50N 90E	completed
2024-08-21T21:51:12	308	SWI_MOON_LIMB_STARE_FS_V1	HCl, HCN	73N	completed
2024-08-21T21:57:12	309	SWI_MOON_LIMB_SCAN_FS_V1	HCl, HCN	Dayside Eq.	completed
2024-08-21T22:02:12	310	SWI_MOON_LIMB_SCAN_FS_V1	HCl, HCN	Nightside Eq.	completed
2024-08-21T22:07:12	311	SWI_2D_MAP_OTF_V1	HCl, HCN	Eq. $\pm 4b$	completed
2024-08-21T22:23:12	312	SWI_2D_MAP_OTF_V1	HCl, HCN	CM $\pm 4b$	completed
2024-08-21T22:39:12	313	SWI_SPECTRAL_SCAN_CTS_FS_V1	8 tunings	Night limb, Eq.	completed
2024-08-21T22:50:12	314	SWI_SPECTRAL_SCAN_CTS_FS_V1	8 tunings	Night limb, Eq.	failed
2024-08-21T23:01	315	SWI_SPECTRAL_SCAN_CTS_FS_V1	8 tunings	Night limb, Eq.	not executed
2024-08-21T23:12	316	SWI_SPECTRAL_SCAN_CTS_FS_V1	8 tunings	Night limb, Eq.	not executed
2024-08-21T23:23	317	SWI_SPECTRAL_SCAN_CTS_FS_V1	8 tunings	Night limb, Eq.	not executed
2024-08-21T23:34	318	SWI_SPECTRAL_SCAN_CTS_FS_V1	8 tunings	Night limb, Eq.	not executed
2024-08-21T23:45	319	SWI_SPECTRAL_SCAN_CTS_FS_V1	8 tunings	Night limb, Eq.	not executed
2024-08-21T23:56	320	SWI_SPECTRAL_SCAN_CTS_FS_V1	8 tunings	Night limb, Eq.	not executed
2024-08-22T00:07	321	SWI_SPECTRAL_SCAN_CTS_FS_V1	8 tunings	Night limb, Eq.	not executed
2024-08-22T02:50	335	SWI_SPECTRAL_SCAN_CTS_FS_V1	8 tunings	South Pole	not executed
2024-08-22T03:02	336	SWI_SPECTRAL_SCAN_CTS_FS_V1	8 tunings	South Pole	not executed
2024-08-22T03:14	337	SWI_SPECTRAL_SCAN_CTS_FS_V1	8 tunings	South Pole	not executed
2024-08-22T03:26	338	SWI_SPECTRAL_SCAN_CTS_FS_V1	8 tunings	South Pole	not executed
2024-08-22T03:38	339	SWI_SPECTRAL_SCAN_CTS_FS_V1	8 tunings	South Pole	not executed
2024-08-22T03:50	340	SWI_SPECTRAL_SCAN_CTS_FS_V1	8 tunings	South Pole	not executed
2024-08-22T04:02	341	SWI_SPECTRAL_SCAN_CTS_FS_V1	8 tunings	South Pole	not executed
2024-08-22T04:14	342	SWI_SPECTRAL_SCAN_CTS_FS_V1	8 tunings	South Pole	not executed
2024-08-22T04:26	343	SWI_SPECTRAL_SCAN_CTS_FS_V1	8 tunings	South Pole	not executed
2024-08-22T04:38	344	SWI_2D_MAP_OTF_V1	O_3, CO, HCN	AT scan $\pm 5b$	not executed
2024-08-22T04:47	345	SWI_2D_MAP_OTF_V1	O_3, CO, HCN	CT scan $\pm 5b$	not executed
2024-08-22T04:55	346	SWI_MOON_LIMB_STARE_FS_V1	O_3, CO, HCN	72S	not executed
2024-08-22T05:04	347	SWI_MOON_LIMB_STARE_FS_V1	O_3, CO, HCN	50S 90W	not executed

Date	ObsID	Obs. mode	LO setup	Comment	Status
2024-08-22T05:13	348	SWI_MOON_LIMB_STARE_FS_V1	O_3, CO, HCN	50S 90E	not executed
2024-08-22T05:22	349	SWI_MOON_LIMB_STARE_FS_V1	O_3, CO, HCN	30S 90W	not executed
2024-08-22T05:31	350	SWI_MOON_LIMB_STARE_FS_V1	O_3, CO, HCN	30S 90E	not executed
2024-08-22T05:40	351	SWI_MOON_LIMB_STARE_FS_V1	O_3, CO, HCN	15S 90W	not executed
2024-08-22T05:49	352	SWI_MOON_LIMB_STARE_FS_V1	O_3, CO, HCN	15S 90E	not executed
2024-08-22T05:58	353	SWI_MOON_LIMB_STARE_FS_V1	O_3, CO, HCN	Eq 90W	not executed
2024-08-22T06:07	354	SWI_MOON_LIMB_STARE_FS_V1	O_3, CO, HCN	Eq 90E	not executed
2024-08-22T06:16	355	SWI_MOON_LIMB_STARE_FS_V1	O_3, CO, HCN	15N 90W	not executed
2024-08-22T06:25	356	SWI_MOON_LIMB_STARE_FS_V1	O_3, CO, HCN	15N 90E	not executed
2024-08-22T06:34	357	SWI_MOON_LIMB_STARE_FS_V1	O_3, CO, HCN	30N 90W	not executed
2024-08-22T06:43	358	SWI_MOON_LIMB_STARE_FS_V1	O_3, CO, HCN	30N 90E	not executed
2024-08-22T06:52	359	SWI_MOON_LIMB_STARE_FS_V1	O_3, CO, HCN	50N 90W	not executed
2024-08-22T07:01	360	SWI_MOON_LIMB_STARE_FS_V1	O_3, CO, HCN	50N 90E	not executed
2024-08-22T07:10	361	SWI_MOON_LIMB_STARE_FS_V1	O_3, CO, HCN	72N	not executed
2024-08-22T07:19	362	SWI_NADIR_STARE_FS_V1	O_3, CO, HCN	Nadir	not executed
2024-08-22T07:48	363	SWI_MOON_LIMB_SCAN_FS_V1	O_3, CO, HCN	Dawn, Eq.	not executed
2024-08-22T07:59	364	SWI_MOON_LIMB_SCAN_FS_V1	O_3, CO, HCN	Dusk, Eq.	not executed
2024-08-22T08:10	365	SWI_MOON_LIMB_SCAN_FS_V1	O_3, CO, HCN	South Pole	not executed
2024-08-22T08:21	366	SWI_MOON_LIMB_SCAN_FS_V1	O_3, CO, HCN	North Pole	not executed
2024-08-22T08:32	367	SWI_2D_MAP_OTF_V1	O_3, CO, HCN	Eq. $\pm 4b$	not executed
2024-08-22T08:46	368	SWI_2D_MAP_OTF_V1	O_3, CO, HCN	CM $\pm 4b$	not executed
2024-08-22T09:00	369	SWI_2D_MAP_OTF_V1	H_2O	15×15 map	not executed
2024-08-22T10:02	370	SWI_2D_MAP_OTF_V1	O_3, O_2	15×15 map	not executed
2024-08-22T11:04	371	SWI_2D_MAP_OTF_V1	HCN, HCl	15×15 map	not executed
2024-08-22T12:06	372	SWI_2D_MAP_OTF_V1	O_3, CO, HCN	15×15 map	not executed
2024-08-22T13:08	373	SWI_2D_MAP_OTF_V1	H_2O, HDO, CS	15×15 map	completed
2024-08-22T14:10:12	374	SWI_2D_MAP_OTF_V1	ClO, H_2O isot.	15×15 map	completed
2024-08-22T15:12:12	375	SWI_2D_MAP_OTF_V1	H_2O, NO, N_2O	15×15 map	completed
2024-08-22T16:14:12	376	SWI_2D_MAP_OTF_V1	O_3, SO, SO_2	15×15 map	completed
2024-08-22T17:16:12	377	SWI_2D_MAP_OTF_V1	O_3, HF	15×15 map	completed
2024-08-22T18:18:12	378	SWI_2D_MAP_OTF_V1	O_3, N_2O, CH_4	15×15 map	completed
2024-08-22T19:20:12	379	SWI_2D_MAP_OTF_V1	H_2O	15×15 map	completed

Date	ObsID	Obs. mode	LO setup	Comment	Status
2024-08-22T20:22:12	380	SWI_2D_MAP_OTF_V1	O_3, H_2O, NO		
2024-08-23T07:00:12	386	SWI_SPECTRAL_SCAN_CTS_PS_V1	11 tunings	Nadir	completed
2024-08-23T07:11:12	387	SWI_SPECTRAL_SCAN_CTS_PS_V1	11 tunings	Nadir	completed
2024-08-23T07:22:12	388	SWI_SPECTRAL_SCAN_CTS_PS_V1	11 tunings	Nadir	completed
2024-08-23T07:33:12	389	SWI_SPECTRAL_SCAN_CTS_PS_V1	11 tunings	Nadir	completed
2024-08-23T07:44:12	390	SWI_SPECTRAL_SCAN_CTS_PS_V1	11 tunings	Nadir	completed
2024-08-23T07:55:12	391	SWI_SPECTRAL_SCAN_CTS_PS_V1	11 tunings	Nadir	completed
2024-08-23T08:06:12	392	SWI_SPECTRAL_SCAN_CTS_FS_V1	8 tunings	Nadir	completed
2024-08-23T08:18:12	393	SWI_SPECTRAL_SCAN_CTS_FS_V1	8 tunings	Nadir	completed
2024-08-23T08:30:12	394	SWI_SPECTRAL_SCAN_CTS_FS_V1	8 tunings	Nadir	completed
2024-08-23T08:42:12	395	SWI_SPECTRAL_SCAN_CTS_FS_V1	8 tunings	Nadir	completed
2024-08-23T08:54:12	396	SWI_SPECTRAL_SCAN_CTS_FS_V1	8 tunings	Nadir	completed
2024-08-23T09:06:12	397	SWI_SPECTRAL_SCAN_CTS_FS_V1	8 tunings	Nadir	completed
2024-08-23T09:18:12	398	SWI_SPECTRAL_SCAN_CTS_FS_V1	8 tunings	Nadir	completed
2024-08-23T09:30:12	399	SWI_SPECTRAL_SCAN_CTS_FS_V1	8 tunings	Nadir	completed
2024-08-23T12:54:11	418	SWI_SPECTRAL_SCAN_ACS_PS_V1	13 tunings	Nadir	completed
2024-08-23T13:10:11	419	SWI_SPECTRAL_SCAN_ACS_PS_V1	13 tunings	Nadir	completed
2024-08-23T13:26:11	420	SWI_SPECTRAL_SCAN_ACS_PS_V1	13 tunings	Nadir	completed
2024-08-23T13:42:11	421	SWI_SPECTRAL_SCAN_ACS_PS_V1	13 tunings	Nadir	completed
2024-08-23T13:58:11	422	SWI_SPECTRAL_SCAN_ACS_PS_V1	13 tunings	Nadir	completed
2024-08-23T14:14:11	423	SWI_SPECTRAL_SCAN_ACS_FS_V1	10 tunings	Nadir	completed
2024-08-23T14:28:11	424	SWI_SPECTRAL_SCAN_ACS_FS_V1	10 tunings	Nadir	completed
2024-08-23T14:42:11	425	SWI_SPECTRAL_SCAN_ACS_FS_V1	10 tunings	Nadir	completed
2024-08-23T14:56:11	426	SWI_SPECTRAL_SCAN_ACS_FS_V1	10 tunings	Nadir	completed
2024-08-23T15:10:11	427	SWI_SPECTRAL_SCAN_ACS_FS_V1	10 tunings	Nadir	completed
2024-08-23T15:24:11	428	SWI_SPECTRAL_SCAN_ACS_FS_V1	10 tunings	Nadir	completed
2024-08-23T18:32:11	440	SWI_SPECTRAL_SCAN_ACS_PS_V1	13 tunings	Nadir	completed
2024-08-23T18:48:11	441	SWI_SPECTRAL_SCAN_ACS_PS_V1	13 tunings	Nadir	completed
2024-08-23T19:04:11	442	SWI_SPECTRAL_SCAN_ACS_PS_V1	13 tunings	Nadir	completed
2024-08-23T19:20:11	443	SWI_SPECTRAL_SCAN_ACS_PS_V1	13 tunings	Nadir	completed
2024-08-23T19:36:11	444	SWI_SPECTRAL_SCAN_ACS_PS_V1	13 tunings	Nadir	completed
2024-08-23T19:52:11	445	SWI_SPECTRAL_SCAN_ACS_PS_V1	13 tunings	Nadir	completed

Date	ObsID	Obs. mode	LO setup	Comment	Status
2024-08-23T20:08:11	446	SWI_SPECTRAL_SCAN_ACS_PS_V1	13 tunings	Nadir	completed
2024-08-23T20:24:11	447	SWI_SPECTRAL_SCAN_ACS_PS_V1	13 tunings	Nadir	completed
2024-08-23T20:40:11	448	SWI_SPECTRAL_SCAN_ACS_PS_V1	13 tunings	Nadir	completed
2024-08-23T20:56:11	449	SWI_SPECTRAL_SCAN_ACS_PS_V1	13 tunings	Nadir	completed
2024-08-23T21:12:11	450	SWI_SPECTRAL_SCAN_ACS_PS_V1	13 tunings	Nadir	completed
2024-08-23T21:28:11	451	SWI_SPECTRAL_SCAN_ACS_PS_V1	13 tunings	Nadir	completed

610 *Author contributions.* T. Cavalié prepared the original manuscript. T. Cavalié, R. Moreno, L. Rezac, C. Jarchow, A. Schulz-Ravanbakhsh, and P. Hartogh defined the LEGA operational strategy for SWI. T. Cavalié and F. Herpin designed the SWI observation modes. T. Cavalié, A. Carrasco Gallardo, L. Rezac, S. Goodyear, and P. Mancini worked out the uplink of SWI observations. All co-authors contributed to the successful implementation of SWI and commented the manuscript.

Competing interests. The authors declare no competing interest.

615 *Acknowledgements.* SWI has been designed and developed by an international consortium of institutes led by the Max Planck Institute for Solar System Research (MPS, Germany) and including the Laboratory for Studies of Radiation and Matter in Astrophysics (LERMA, France), the Space Research Centre of the Polish Academy of Sciences (CBK, Poland), Chalmers University of Technology (Sweden), the Institute of Applied Physics of the University of Bern (IAP, Switzerland), the National Institute of Information and Communications Technology (NICT, Japan) and the French Space Agency CNES with additional support from the Laboratoire d'Instrumentation et de Recherche en
620 Astrophysique of the Observatoire de Paris (LIRA, France), the Laboratoire d'Astrophysique de Bordeaux (LAB, France), the RPG Radiometer Physics GmbH (Germany), and Omnisys Instrument AV (Sweden). This development has been supported by national funding agencies and other organizations, including the Deutsches Zentrum für Luft- und Raumfahrt (DLR) and by central resources of the Max-Planck-Society. T. Cavalié, F. Herpin, and P. Mancini, acknowledge funding from the Centre National d'Études Spatiales (CNES). E.S. Wirström acknowledges generous support from the Swedish National Space Agency. Juice is a mission under ESA leadership with contributions from
625 its Member States, NASA, JAXA, and the Israel Space Agency. It is the first Large-class mission in ESA's Cosmic Vision Program.

References

Altobelli, N., Vallat, C., and Witasse, O.: Title TBD, Ann. Geophys., ??, ??, 2026.

Benmahi, B., Cavalié, T., Fouchet, T., Moreno, R., Lellouch, E., Bardet, D., Guerlet, S., Hue, V., and Spiga, A.: First absolute wind measurements in Saturn's stratosphere from ALMA observations, Astron. Astrophys., 666, A117, https://doi.org/10.1051/0004-6361/202244200, 2022.

Benmahi, B., Cavalié, T., Fouchet, T., Moreno, R., Lellouch, E., Bardet, D., Guerlet, S., Hue, V., and Spiga, A.: First absolute wind measurements in Saturn's stratosphere from ALMA observations (Corrigendum), Astron. Astrophys., 696, C5, https://doi.org/10.1051/0004-6361/202554767e, 2025.

Biver, N., Hofstadter, M., Gulkis, S., Bockelée-Morvan, D., Choukroun, M., Lellouch, E., Schloerb, F. P., Rezac, L., Ip, W. H., Jarchow, C., Hartogh, P., Lee, S., von Allmen, P., Crovisier, J., Leyrat, C., and Encrenaz, P.: Distribution of water around the nucleus of comet 67P/Churyumov-Gerasimenko at 3.4 AU from the Sun as seen by the MIRO instrument on Rosetta, Astron. Astrophys., 583, A3, https://doi.org/10.1051/0004-6361/201526094, 2015.

Boissinot, A., Spiga, A., Guerlet, S., Cabanes, S., and Bardet, D.: Global climate modeling of the Jupiter troposphere and effect of dry and moist convection on jets, Astron. Astrophys., 687, A274, https://doi.org/10.1051/0004-6361/202245220, 2024.

Boutonnet, A., Langevin, Y., and Erd, C.: Designing the JUICE Trajectory, Space Sci. Rev., 220, 67, https://doi.org/10.1007/s11214-024-01093-y, 2024.

Carrión-González, Ó., Moreno, R., Lellouch, E., Cavalié, T., Guerlet, S., Milcareck, G., Spiga, A., Clément, N., and Leconte, J.: Doppler wind measurements in Neptune's stratosphere with ALMA, Astron. Astrophys., 674, L3, https://doi.org/10.1051/0004-6361/202346621, 2023.

Cavalié, T., Billebaud, F., Biver, N., Dobrijevic, M., Lellouch, E., Brillet, J., Lecacheux, A., Hjalmarson, Å., Sandqvist, A., Frisk, U., Olberg, M., Bergin, E. A., and The Odin Team: Observation of water vapor in the stratosphere of Jupiter with the Odin space telescope, Planet. Space Sci., 56, 1573–1584, https://doi.org/10.1016/j.pss.2008.04.013, 2008.

Cavalié, T., Feuchtgruber, H., Lellouch, E., de Val-Borro, M., Jarchow, C., Moreno, R., Hartogh, P., Orton, G., Greathouse, T. K., Billebaud, F., Dobrijevic, M., Lara, L. M., González, A., and Sagawa, H.: Spatial distribution of water in the stratosphere of Jupiter from Herschel HIFI and PACS observations, Astron. Astrophys., 553, A21, https://doi.org/10.1051/0004-6361/201220797, 2013.

Cavalié, T., Moreno, R., Lellouch, E., Hartogh, P., Venot, O., Orton, G. S., Jarchow, C., Encrenaz, T., Selsis, F., Hersant, F., and Fletcher, L. N.: The first submillimeter observation of CO in the stratosphere of Uranus, Astron. Astrophys., 562, A33, https://doi.org/10.1051/0004-6361/201322297, 2014.

Cavalié, T., Benmahi, B., Hue, V., Moreno, R., Lellouch, E., Fouchet, T., Hartogh, P., Rezac, L., Greathouse, T. K., Gladstone, G. R., Sinclair, J. A., Dobrijevic, M., Billebaud, F., and Jarchow, C.: First direct measurement of auroral and equatorial jets in the stratosphere of Jupiter, Astron. Astrophys., 647, L8, https://doi.org/10.1051/0004-6361/202140330, 2021.

Cavalié, T., Rezac, L., Moreno, R., Lellouch, E., Fouchet, T., Benmahi, B., Greathouse, T. K., Sinclair, J. A., Hue, V., Hartogh, P., Dobrijevic, M., Carrasco, N., and Perrin, Z.: Evidence for auroral influence on Jupiter's nitrogen and oxygen chemistry revealed by ALMA, Nature Astronomy, 7, 1048–1055, https://doi.org/10.1038/s41550-023-02016-7, 2023.

Costagliola, F., Sakamoto, K., Muller, S., Martín, S., Aalto, S., Harada, N., van der Werf, P., Viti, S., Garcia-Burillo, S., and Spaans, M.: Exploring the molecular chemistry and excitation in obscured luminous infrared galaxies. An ALMA mm-wave spectral scan of NGC 4418, Astron. Astrophys., 582, A91, https://doi.org/10.1051/0004-6361/201526256, 2015.

De Beck, E. and Olofsson, H.: Circumstellar environment of the M-type AGB star R Doradus. APEX spectral scan at 159.0-368.5 GHz, Astron. Astrophys., 615, A8, https://doi.org/10.1051/0004-6361/201732470, 2018.

665 de Kleer, K., Butler, B., de Pater, I., Gurwell, M. A., Moullet, A., Trumbo, S., and Spencer, J.: Ganymede's Surface Properties from Millimeter and Infrared Thermal Emission, Plan. Sci. J., 2, 5, https://doi.org/10.3847/PSJ/abcbf4, 2021.

de Pater, I., Goldstein, D., and Lellouch, E.: The Plumes and Atmosphere of Io, in: Io: A New View of Jupiter's Moon, edited by Lopes, R. M. C., de Kleer, K., and Keane, J. T., vol. 468 of *Astrophysics and Space Science Library*, pp. 233–290, https://doi.org/10.1007/978-3-031-25670-7_8, 2023.

670 Gallardo Cava, I., Alcolea, J., Bujarrabal, V., Gómez-Garrido, M., and Castro-Carrizo, A.: The nebula around the binary post-AGB star 89 Herculis, Astron. Astrophys., 671, A80, https://doi.org/10.1051/0004-6361/202244415, 2023.

Gapp, C., Rengel, M., Hartogh, P., Sagawa, H., Feuchtgruber, H., Lellouch, E., and Villanueva, G. L.: Abundances of trace constituents in Jupiter's atmosphere inferred from Herschel/PACS observations, Astron. Astrophys., 688, A10, https://doi.org/10.1051/0004-6361/202347345, 2024.

675 Grasset, O., Dougherty, M. K., Coustenis, A., Bunce, E. J., Erd, C., Titov, D., Blanc, M., Coates, A., Drossart, P., Fletcher, L. N., Hussmann, H., Jaumann, R., Krupp, N., Lebreton, J.-P., Prieto-Ballesteros, O., Tortora, P., Tosi, F., and Van Hoolst, T.: JUpiter ICy moons Explorer (JUICE): An ESA mission to orbit Ganymede and to characterise the Jupiter system, Planet. Space Sci., 78, 1–21, https://doi.org/10.1016/j.pss.2012.12.002, 2013.

Guerlet, S., Fouchet, T., Spiga, A., Flasar, F. M., Fletcher, L. N., Hesman, B. E., and Gorius, N.: Equatorial Oscillation and Planetary Wave
680 Activity in Saturn's Stratosphere Through the Cassini Epoch, J. Geophys. Res., 123, 246–261, https://doi.org/10.1002/2017JE005419, 2018.

Guerlet, S., Spiga, A., Delattre, H., and Fouchet, T.: Radiative-equilibrium model of Jupiter's atmosphere and application to estimating stratospheric circulations, Icarus, 351, 113935, https://doi.org/10.1016/j.icarus.2020.113935, 2020.

Gulkis, S., Frerking, M., Crovisier, J., Beaudin, G., Hartogh, P., Encrenaz, P., Koch, T., Kahn, C., Salinas, Y., Nowicki, R., Irigoyen, R.,
685 Janssen, M., Stek, P., Hofstadter, M., Allen, M., Backus, C., Kamp, L., Jarchow, C., Steinmetz, E., Deschamps, A., Krieg, J., Gheudin, M., Bockelée-Morvan, D., Biver, N., Encrenaz, T., Despois, D., Ip, W., Lellouch, E., Mann, I., Muhleman, D., Rauer, H., Schloerb, P., and Spilker, T.: MIRO: Microwave Instrument for Rosetta Orbiter, Space Sci. Rev., 128, 561–597, https://doi.org/10.1007/s11214-006-9032-y, 2007.

Hartogh, P., Crovisier, J., de Val-Borro, M., Bockelée-Morvan, D., Biver, N., Lis, D. C., Moreno, R., Jarchow, C., Rengel, M., Emprechtinger,
690 M., Szutowicz, S., Banaszkiewicz, M., Bensch, F., Blecka, M. I., Cavalié, T., Encrenaz, T., Jehin, E., Küppers, M., Lara, L.-M., Lellouch, E., Swinyard, B. M., Vandenbussche, B., Bergin, E. A., Blake, G. A., Blommaert, J. A. D. L., Cernicharo, J., Decin, L., Encrenaz, P., de Graauw, T., Hutsemekers, D., Kidger, M., Manfroid, J., Medvedev, A. S., Naylor, D. A., Schieder, R., Thomas, N., Waelkens, C., Roelfsema, P. R., Dieleman, P., Güsten, R., Klein, T., Kasemann, C., Caris, M., Olberg, M., and Benz, A. O.: HIFI observations of water in the atmosphere of comet C/2008 Q3 (Garradd), Astron. Astrophys., 518, L150, https://doi.org/10.1051/0004-6361/201014665, 2010a.

695 Hartogh, P., Jarchow, C., Lellouch, E., de Val-Borro, M., Rengel, M., Moreno, R., Medvedev, A. S., Sagawa, H., Swinyard, B. M., Cavalié, T., Lis, D. C., Błęcka, M. I., Banaszkiewicz, M., Bockelée-Morvan, D., Crovisier, J., Encrenaz, T., Küppers, M., Lara, L.-M., Szutowicz, S., Vandenbussche, B., Bensch, F., Bergin, E. A., Billebaud, F., Biver, N., Blake, G. A., Blommaert, J. A. D. L., Cernicharo, J., Decin, L., Encrenaz, P., Feuchtgruber, H., Fulton, T., de Graauw, T., Jehin, E., Kidger, M., Lorente, R., Naylor, D. A., Portyankina, G., Sánchez-Portal, M., Schieder, R., Sidher, S., Thomas, N., Verdugo, E., Waelkens, C., Whyborn, N., Teyssier, D., Helmich, F., Roelfsema, P., Stutzki,

700   J., Leduc, H. G., and Stern, J. A.: Herschel/HIFI observations of Mars: First detection of O_2 at submillimetre wavelengths and upper limits on HCl and H_2O_2, Astron. Astrophys., 521, L49, https://doi.org/10.1051/0004-6361/201015160, 2010b.

Hartogh, P., Lellouch, E., Rezac, L., and others: Submillimetre Wave Instrument (SWI) on board ESA's Jupiter Icy Moons Explorer (JUICE), Space Sci. Rev., in prep, 2026a.

Hartogh, P., Rezac, L., and others: The 2024 Lunar-Earth Gravity Assist as seen by SWI/JUICE: Overview, Ann. Geophys., ??, ??, 2026b.

705   Jarchow, C., Rezac, L., Hartogh, P., Schulz-Ravanbakhsh, A., Cavalié, T., and Moreno, R.: Observations of the Earth as Calibration Target for JUICE/SWI during the Lunar-Earth-Gravity-Assist, Ann. Geophys., ??, ??, 2026.

King, O. R. T. and Fletcher, L. N.: PlanetMapper: A Python package for visualising, navigating and mapping Solar System observations, Journal of Open Source Software, 8, 5728, https://doi.org/10.21105/joss.05728, 2023.

Lefour, C., Cavalié, T., Moreno, R., Rezac, L., Fouchet, T., Lellouch, E., and Hartogh, P.: New $^{12}C/^{13}C$ and $^{15}N/^{14}N$ isotopic ratios mea-
710   surements in HCN in the Jupiter stratosphere revealed by ALMA, Astron. Astrophys., in prep., 2026.

Livengood, T. A., Chin, G., Sagdeev, R. Z., Mitrofanov, I. G., Boynton, W. V., Evans, L. G., Litvak, M. L., McClanahan, T. P., Sanin, A. B., Starr, R. D., and Su, J. J.: Moonshine: Diurnally varying hydration through natural distillation on the Moon, detected by the Lunar Exploration Neutron Detector (LEND), Icarus, 255, 100–115, https://doi.org/10.1016/j.icarus.2015.04.004, 2015.

Marconi, M. L.: A kinetic model of Ganymede's atmosphere, Icarus, 190, 155–174, https://doi.org/10.1016/j.icarus.2007.02.016, 2007.

715   Medvedev, A. S., Sethunadh, J., and Hartogh, P.: From cold to warm gas giants: A three-dimensional atmospheric general circulation modeling, Icarus, 225, 228–235, https://doi.org/10.1016/j.icarus.2013.03.028, 2013.

Moreno, R., Jarchow, C., Fomanek, T., and others: Pointing and beam characterization of JUICE/SWI during the Lunar-Earth Gravity Assist, Ann. Geophys., ??, ??, 2026.

Moses, J. I., Fouchet, T., Bézard, B., Gladstone, G. R., Lellouch, E., and Feuchtgruber, H.: Photochemistry and diffusion in
720   Jupiter's stratosphere: Constraints from ISO observations and comparisons with other giant planets, J. Geophys. Res., 110, E08001, https://doi.org/10.1029/2005JE002411, 2005.

Mousis, O., Lunine, J. I., Fletcher, L. N., Mandt, K. E., Ali-Dib, M., Gautier, D., and Atreya, S.: New Insights on Saturn's Formation from its Nitrogen Isotopic Composition, Astrophys. J. Lett., 796, L28, https://doi.org/10.1088/2041-8205/796/2/L28, 2014.

Olberg, M., Frisk, U., Lecacheux, A., Olofsson, A. O. H., Baron, P., Bergman, P., Florin, G., Hjalmarson, Å. ., Larsson, B., Murtagh, D.,
725   Olofsson, G., Pagani, L., Sandqvist, A., Teyssier, D., Torchinsky, S. A., and Volk, K.: The Odin satellite. II. Radiometer data processing and calibration, Astron. Astrophys., 402, L35–L38, https://doi.org/10.1051/0004-6361:20030336, 2003.

Ossenkopf, V.: Optimization of mapping modes for heterodyne instruments, Astron. Astrophys., 495, 677–690, https://doi.org/10.1051/0004-6361:200809619, 2009.

Rezac, L. and et al.: Moon flyby observations of JUICE/SWI during the first Earth Moon gravity assist, Ann. Geophys., in prep, 2026.

730   Roelfsema, P. R., Helmich, F. P., Teyssier, D., Ossenkopf, V., Morris, P., Olberg, M., Shipman, R., Risacher, C., Akyilmaz, M., Assendorp, R., Avruch, I. M., Beintema, D., Biver, N., Boogert, A., Borys, C., Braine, J., Caris, M., Caux, E., Cernicharo, J., Coeur-Joly, O., Comito, C., de Lange, G., Delforge, B., Dieleman, P., Dubbeldam, L., de Graauw, T., Edwards, K., Fich, M., Flederus, F., Gal, C., di Giorgio, A., Herpin, F., Higgins, D. R., Hoac, A., Huisman, R., Jarchow, C., Jellema, W., de Jonge, A., Kester, D., Klein, T., Kooi, J., Kramer, C., Laauwen, W., Larsson, B., Leinz, C., Lord, S., Lorenzani, A., Luinge, W., Marston, A., Martín-Pintado, J., McCoey, C., Melchior, M.,
735   Michalska, M., Moreno, R., Müller, H., Nowosielski, W., Okada, Y., Orleański, P., Phillips, T. G., Pearson, J., Rabois, D., Ravera, L., Rector, J., Rengel, M., Sagawa, H., Salomons, W., Sánchez-Suárez, E., Schieder, R., Schlöder, F., Schmülling, F., Soldati, M., Stutzki, J., Thomas, B., Tielens, A. G. G. M., Vastel, C., Wildeman, K., Xie, Q., Xilouris, M., Wafelbakker, C., Whyborn, N., Zaal, P., Bell, T.,

Bjerkeli, P., De Beck, E., Cavalié, T., Crockett, N. R., Hily-Blant, P., Kama, M., Kaminski, T., Leflóch, B., Lombaert, R., de Luca, M., Makai, Z., Marseille, M., Nagy, Z., Pacheco, S., van der Wiel, M. H. D., Wang, S., and Yıldız, U.: In-orbit performance of Herschel-HIFI,
740   Astron. Astrophys., 537, A17, https://doi.org/10.1051/0004-6361/201015120, 2012.

Schieder, R. and Kramer, C.: Optimization of heterodyne observations using Allan variance measurements, Astron. Astrophys., 373, 746–756, https://doi.org/10.1051/0004-6361:20010611, 2001.

Stephan, K., Roatsch, T., Tosi, F., Matz, K.-D., Kersten, E., Wagner, R., Molyneux, P., Palumbo, P., Poulet, F., Hussmann, H., Barabash, S., Bruzzone, L., Dougherty, M., Gladstone, R., Gurvits, L. I., Hartogh, P., Iess, L., Wahlund, J.-E., Wurz, P., Witasse, O., Grasset, O.,
745   Altobelli, N., Carter, J., Cavalié, T., D'Aversa, E., Della Corte, V., Filacchione, G., Galli, A., Galluzzi, V., Gwinner, K., Hauber, E., Jaumann, R., Krohn, K., Langevin, Y., Lucchetti, A., Migliorini, A., Piccioni, G., Solomonidou, A., Stark, A., Tobie, G., Tubiana, C., Vallat, C., van Hoolst, T., and The Juice Swt Team: Regions of interest on Ganymede's and Callisto's surfaces as potential targets for ESA's JUICE mission, Planet. Space Sci., 208, 105324, https://doi.org/10.1016/j.pss.2021.105324, 2021.

Szabó, Z. M., Belloche, A., Menten, K. M., Gong, Y., Kóspál, Á., Ábrahám, P., Yang, W., Cyganowski, C. J., and Wyrowski, F.: Molecular
750   inventory of the environment of a young eruptive star: Case study of the classical FU Orionis star V1057 Cyg, Astron. Astrophys., 694, A329, https://doi.org/10.1051/0004-6361/202451851, 2025.

Tolls, V., Melnick, G. J., Ashby, M. L. N., Bergin, E. A., Gurwell, M. A., Kleiner, S. C., Patten, B. M., Plume, R., Stauffer, J. R., Wang, Z., Zhang, Y. F., Chin, G., Erickson, N. R., Snell, R. L., Goldsmith, P. F., Neufeld, D. A., Schieder, R., and Winnewisser, G.: Submillimeter Wave Astronomy Satellite Performance on the ground and in orbit, Astrophys. J. Suppl. Ser., 152, 137–162,
755   https://doi.org/10.1086/382507, 2004.

Wirstrom, E. S., Bjerkeli, P., Rezac, L., Brinch, C., and Hartogh, P.: Effect of the 3D distribution on water observations made with the SWI - I. Ganymede, Astron. Astrophys., 637, A90, https://doi.org/10.1051/0004-6361/202037609, 2020.